Petroleum Science 20 (2023) 2921–2938

Contents lists available at ScienceDirect

Petroleum Science

journal homepage: www.keaipublishing.com/en/journals/petroleum-science

Original Paper

Optimization of operational strategies for rich gas enhanced oil recovery based on a pilot test in the Bakken tight oil reservoir

Xincheng Wan*, Lu Jin, Nicholas A. Azzolina, Jin Zhao, Xue Yu, Steven A. Smith, James A. Sorensen

Energy & Environmental Research Center, University of North Dakota, 15 North 23rd Street, Stop 9018, Grand Forks, ND, 58202-9018, USA

ARTICLE INFO

Article history:
Received 29 August 2022
Received in revised form
28 March 2023
Accepted 19 April 2023
Available online 20 April 2023

Edited by Yan-Hua Sun

Keywords:
Rich gas injection
Bakken tight oil reservoir
EOR strategies
Conformance control
Embedded discrete fracture model

ABSTRACT

Horizontal well drilling and multistage hydraulic fracturing have been demonstrated as effective approaches for stimulating oil production in the Bakken tight oil reservoir. However, after multiple years of production, primary oil recovery in the Bakken is generally less than 10% of the estimated original oil in place. Gas huff 'n' puff (HnP) has been tested in the Bakken Formation as an enhanced oil recovery (EOR) method; however, most field pilot test results showed no significant incremental oil production. One of the factors affecting HnP EOR performance is premature gas breakthrough, which is one of the most critical issues observed in the field because of the presence of interwell fractures. Consequently, injected gas rapidly reaches adjacent production wells without contacting reservoir rock and increasing oil recovery. Proper conformance control is therefore needed to avoid early gas breakthrough and improve EOR performance. In this study, a rich gas EOR pilot in the Bakken was carefully analyzed to collect the essential reservoir and operational data. A simulation model with 16 wells was then developed to reproduce the production history and predict the EOR performance with and without conformance control. EOR operational strategies, including single- and multiple-well HnP, with different gas injection constraints were investigated. The simulation results of single-well HnP without conformance control showed that a rich gas injection rate of at least 10 MMscfd was needed to yield meaningful incremental oil production. The strategy of conformance control via water injection could significantly improve oil production in the HnP well, but injecting an excessive amount of water also leads to water breakthrough and loss of oil production in the offset wells. By analyzing the production performance of the wells individually, the arrangement of wells was optimized for multiple-well HnP EOR. The multiwell results showed that rich gas EOR could improve oil production up to 7.4% by employing conformance control strategies. Furthermore, replacing rich gas with propane as the injection gas could result in 14% of incremental oil production.

1. Introduction

Horizontal well drilling and multistage hydraulic fracturing techniques have been widely employed by operators to develop unconventional reservoirs (Pearson et al., 2018; Yu and Sepehrnoori, 2014). The techniques have contributed to a significant amount of oil production in the United States since 2009. The multistage hydraulic fracturing treatment allows operators to access oil in an ultra-low permeability reservoir matrix via multiple high-conductivity hydraulic fractures with a half-length of hundreds of feet. The Bakken petroleum system (Bakken) of the Williston Basin has been one of the most active and prolific unconventional oil plays in the United States. The U.S. Energy Information Administration reported that the total oil production in the Bakken region was 1.1 million barrels/day (bpd) in December 2021 and the average oil production rate for new wells in the Bakken region was 2148 barrels/day (Energy Information Administration, 2021).

Despite the fact that horizontal well drilling and multistage hydraulic fracturing have made a significant impact on improving oil production, the primary oil recovery is still low in the Bakken, typically less than 10% (Hoffman and Evans, 2016; Jin et al., 2017a,

* Corresponding author.
E-mail address: xwan@undeerc.org (X. Wan).

https://doi.org/10.1016/j.petsci.2023.04.018

2017b). To improve oil recovery, techniques are needed to access the remaining oil in the tight rock matrix. Drilling infill wells is an option for operators to extract more oil from the tight reservoir. However, the overall oil production performance of the infill (or child) wells is typically inferior to that of the parent wells. When the oil price is low, the cost of drilling infill wells is difficult to be compensated by the additional oil production (Castro-Alvarez et al., 2018).

Gas injection enhanced oil recovery (EOR) has been increasingly studied to develop unconventional reservoirs. The mechanism of gas injection EOR is that gas would be miscible with oil during injection, contributing to the expansion of oil volume, reduction of oil viscosity, and possible vaporization of oil, which together mobilize the oil from the rock matrix into the fracture network and, thus, additional oil can be produced (Burrows et al., 2020). Laboratory experiments and numerical simulations have been performed to investigate the effectiveness of gas injection for improving oil recovery in tight reservoirs (Ganjdanesh et al., 2020; Hawthorne et al., 2020, 2021; He et al., 2022; Hoffman, 2012; Jin et al., 2022a, 2022b; Li et al., 2019; Pankaj et al., 2018; Shoaib and Hoffman, 2009; Sorensen et al., 2017, 2018; Wan et al., 2022; Wang et al., 2010; Zhang et al., 2021). Gas injection EOR using CO_2 or rich gas has been successfully implemented in numerous conventional reservoirs for decades (Alvarado and Manrique, 2010; Barajas-Olalde et al., 2021; Hawthorne et al., 2016; Jin et al., 2018a, 2018b). Recently, the technique has been successfully employed in the Eagle Ford shale oil play (Hoffman, 2018; Malo et al., 2019). However, the application of gas injection EOR in the Bakken is still in the early stage. Although pilot tests were successful in terms of injecting CO_2 and produced gas into the ultra-low permeability Bakken Formation using both single- and multiple-well huff-n-puff (HnP), little or limited incremental oil was observed in the pilots. Early gas breakthrough was observed in most of the pilots, and it was diagnosed as one of the most critical issues in the EOR process (Hoffman and Evans, 2016; Pospisil et al., 2020; Sorensen and Hamling, 2015; Sorensen et al., 2018; Torres et al., 2019). The results of the pilot tests indicated that interwell fractures with high permeability were present in the reservoir and, therefore, a proper conformance control design was necessary to minimize the impact of these interwell fractures and improve the utilization efficiency of the injected gas (Hoffman and Evans, 2016; Jia et al., 2020, 2021; Pospisil et al., 2020).

To improve the EOR performance, the well bottomhole pressure (BHP) is required to be high enough so that the injected gas can penetrate the tight matrix. However, the previous pilots showed that the BHP in most of the HnP wells was substantially lower than the desired level (Hoffman and Evans, 2016; Pospisil et al., 2020). Since BHP is a function of gas injection rate, the results implied that a much higher gas injection rate was required for future gas injection applications in the Bakken. Water alternating gas (WAG) is a technique that has been proven effective to improve gas sweep efficiency for gas EOR in conventional reservoirs (Alvarado and Manrique, 2010; Hawthorne et al., 2018; Kumar and Mandal, 2017; Salako et al., 2018; Smith et al., 2018). The technique could potentially be implemented in the Bakken to provide pressure support and improve the conformance of gas injection. The challenge is that the complex fractures in the reservoir may complicate the WAG process (Hoffman and Evans, 2016; Zhao et al., 2022).

To optimize the gas injection strategy for EOR in the Bakken, a recently completed EOR pilot test was selected to provide baseline data for this study (Pospisil et al., 2020). HnP simulations with and without conformance control via water injection were performed to evaluate the importance of conformance control on EOR performance. The embedded discrete fracture modeling (EDFM) method was employed to create fractures while a compositional reservoir simulator (Computer Modelling Group's [CMG's] GEM, 2020) was used for flow computation. A reservoir model with 16 wells was constructed and calibrated with production data. The well interference effect was captured using the connected fractures. The model made it possible to investigate the effect of conformance control on EOR performance when multiple wells are used for HnP simultaneously. Based on the history-matched model, a variety of EOR scenarios were studied for single- and multiple-well HnP to optimize the operational strategies in the Bakken.

2. A rich gas EOR pilot in the Bakken

The pilot site is located in Williams County, North Dakota. The reservoir in this pilot site contains the Bakken and Three Forks (TF) Formations, which can be further divided into four intervals with different geologic properties, as shown in Fig. 1. The reservoir structure is typical in the Bakken: the Upper Bakken (UB) and Lower Bakken (LB) intervals are shales, while the Middle Bakken (MB) and TF intervals are tight matrices with mixed layers of mudstone, sandstone, and dolostone (Gaswirth and Marra, 2014; Hawthorne et al., 2017; Jin et al., 2016; Rivero et al., 2018; Smith and Bustin, 1995). The well logs, shown in Fig. 1, and core measurements were used to characterize the reservoir properties, such as porosity and fluid saturations of the intervals.

The basic well information and fracturing data for the 16 wells in the pilot site are summarized in Tables 1 and 2, respectively. All parent and child wells are currently active. Their spatial distribution is illustrated in Fig. 2. Well interference effects were clearly observed in the parent wells when child wells were stimulated for production. Fig. 3 illustrates the significant increase of water cut in parent wells 2TFH and 3MBH when the offset child wells were stimulated for production. This example indicated that there was a strong connectivity between the parent and child wells. The well interference effects were widely observed in the Bakken and other main unconventional plays (Jin et al., 2022a, 2022b; Yu et al., 2020; Zhao et al., 2022).

The oil production rates in some of the wells dropped over 90% after 5 years of production, therefore, rich gas HnP operations were performed to improve the oil production in this site. Five of the 16 wells were used for HnP EOR in the pilot test from July 2018 to May 2019. Rich gas was sequentially injected into 3TFH, 2MBH, 5MBH, 4MBH, and 6TFH, with a cumulative total injection volume of 10.8, 13.8, 41.7, 74, and 17 MMscf, respectively. Because of the compressor capacity, the maximum gas injection rate that could be achieved was 2.5 MMscfd for each well. The BHP response with gas injection in each well is shown in Fig. 4 (Pospisil et al., 2020). BHP in Wells 2MBH and 3TFH increased more rapidly than in the other three wells. One possible reason is that Wells 2MBH and 3TFH have fewer fracture stages (35 vs. 50) so that the injected gas could fill the depleted reservoir volume faster and then lift the pressure.

The BHP of all the injection wells was below the minimum miscibility pressure (MMP) of 2450 psi for rich gas during the injection period because of the limitation of the gas injection rate. Quick gas breakthrough was observed, as evidenced by a gas tracer and an increase of the gas-to-oil ratio in the offset production wells. The goal of rich gas injection was to boost reservoir pressure around the injectors above MMP for a miscible EOR. However, a rapid gas breakthrough combined with the limitations of the gas injection rate made it challenging to boost the pressure in the reservoir. As a result, the EOR effect on production was not encouraging during the test.

Fig. 5 shows an example of EOR production response in Well 3TFH when rich gas was injected into Wells 3TFH (Cycle 1: 07/03/2018–07/14/2018, Cycle 2: 09/03/2018–09/10/2018) and 4MBH (Cycle 1: 01/16/2019–01/29/2019, Cycle 2: 03/13/2019–04/07/

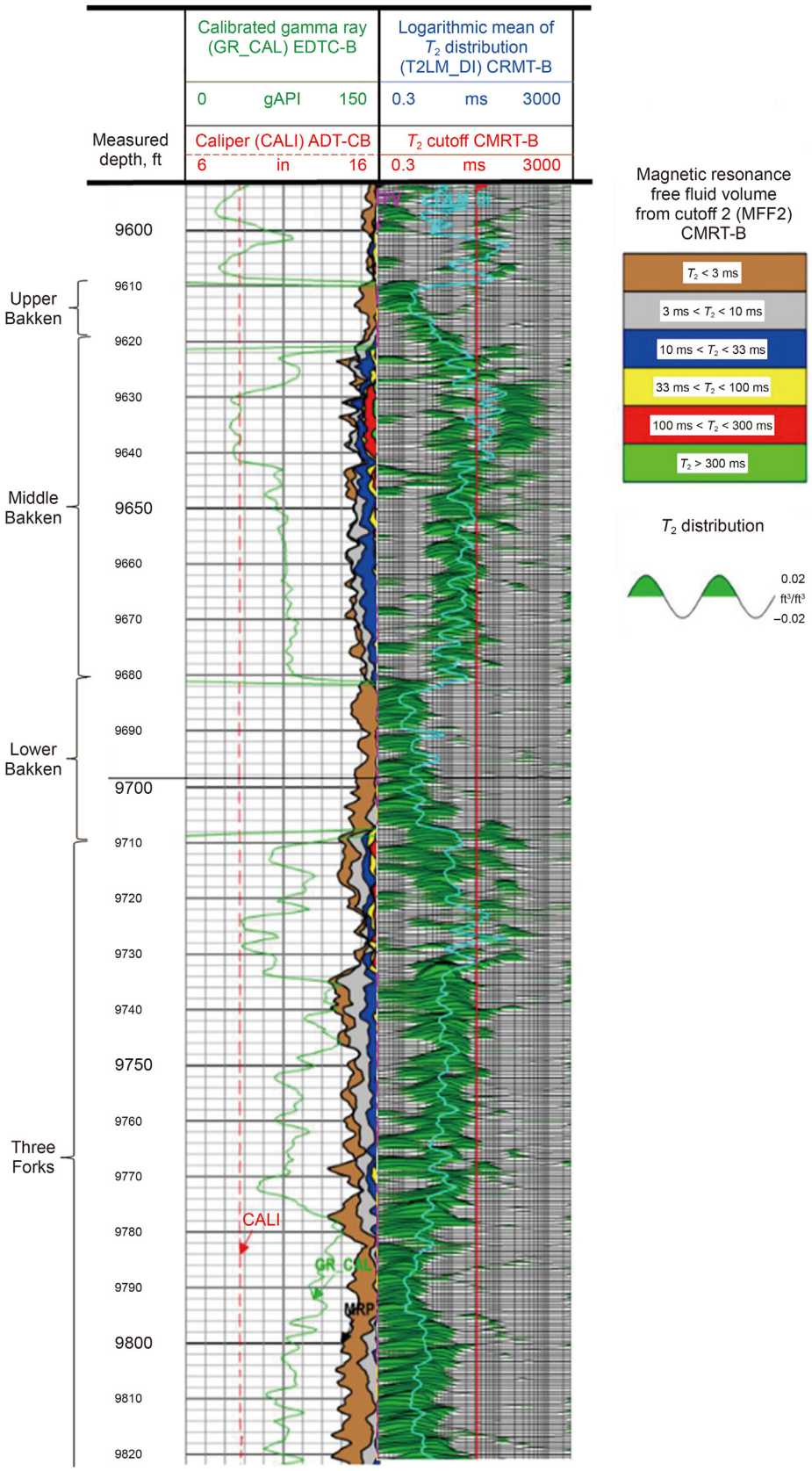

Fig. 1. Well logs measured from one of the EOR wells in the pilot test. The logs show the distribution of geologic intervals in the Bakken and TF Formations.

Table 1
Wells in the pilot site.

No.	Well name	Completed formation/unit	Well type	Lateral length, ft	Well depth, ft	Production start time
1	1TFH	TF	Child	9729	9684	2016
2	1MBH	MB	Child	9564	9591	2016
3	2TFH	TF	Parent	9741	9676	2013
4	2MBH	MB	Child	9792	9589	2016
5	3MBH	MB	Parent	9538	9585	2013
6	3TFH	TF	Child	9763	9679	2016
7	4MBH	MB	Parent	9566	9599	2014
8	5TFH	TF	Parent	9529	9701	2014
9	5MBH	MB	Parent	9617	9587	2014
10	6TFH	TF	Child	9773	9674	2015
11	6MBH	MB	Child	9719	9575	2015
12	10TFH	TF	Child	9501	9664	2015
13	11MBH	MB	Parent	9922	9547	2013
14	11TFH	TF	Child	9573	9658	2015
15	12MBH	MB	Child	9547	9561	2015
16	12TFH	TF	Child	9469	9647	2015

Table 2
Fracturing data for the simulated wells.

Well	Frac. start date	Number of stages	Frac. fluid volume, 10^3 bbl	Proppant amount, MMlb
1TFH	01/2016	35	154	4.7
1MBH	01/2016	35	143	4.7
2TFH	07/2013	33	64	3.0
2MBH	01/2016	35	156	4.7
3MBH	07/2013	33	64	2.9
3TFH	01/2016	35	162	4.7
4MBH	10/2014	50	176	4.1
5TFH	10/2014	50	192	3.9
5MBH	11/2014	50	194	4.2
6TFH	11/2014	50	204	3.9
6MBH	11/2014	50	194	4
10TFH	03/2015	35	172	3.9
11MBH	10/2013	35	61	28
11TFH	03/2015	35	172	4
12MBH	03/2015	35	157	3.9
12TFH	03/2015	35	168	3.9

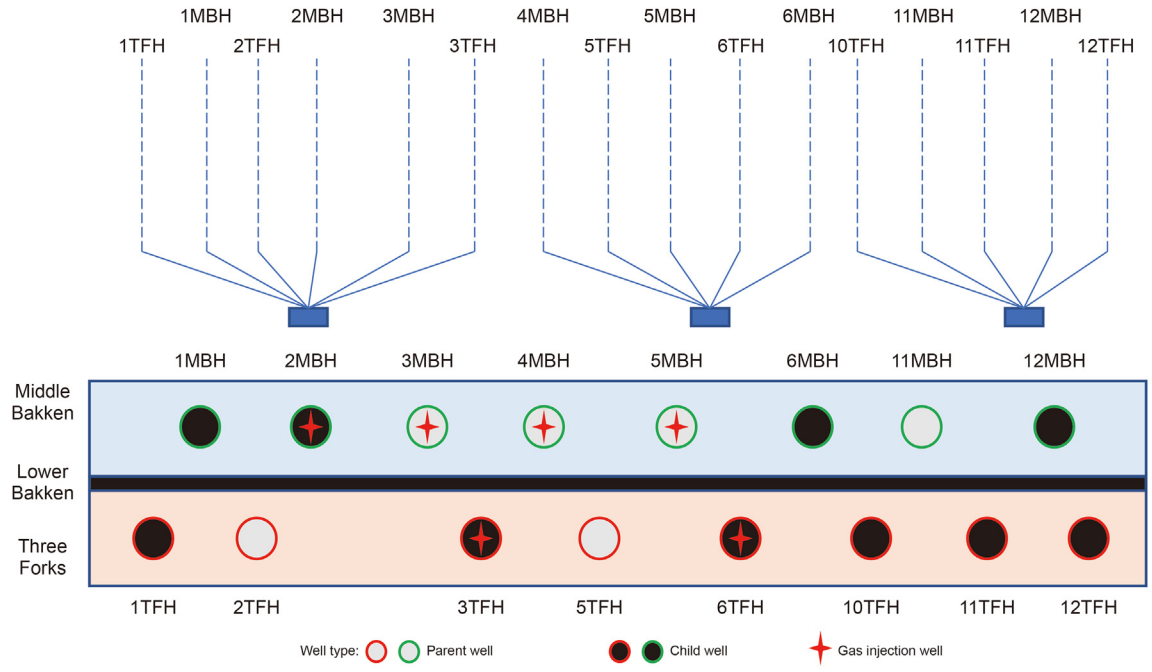

Fig. 2. Schematic of well distribution in the pilot site.

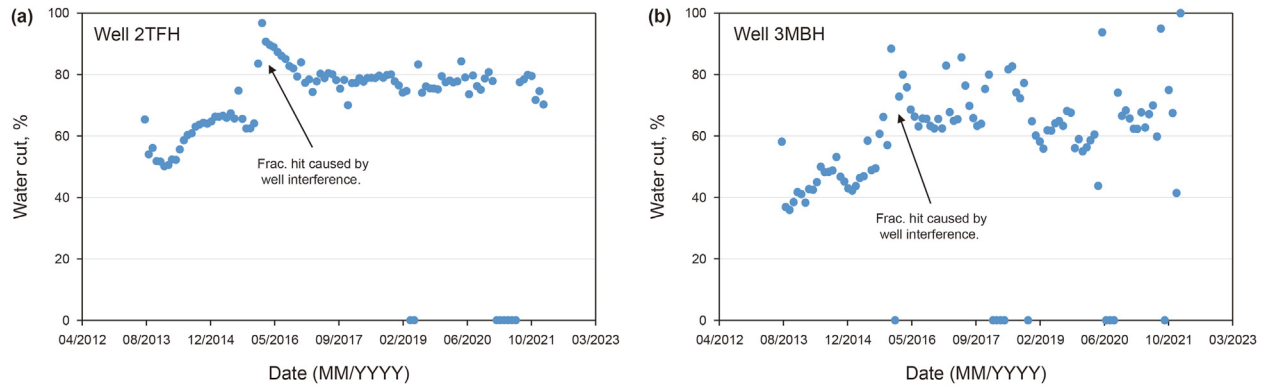

Fig. 3. Illustration of well interference effects in the parent wells (**a**) 2TFH and (**b**) 3MBH when child wells were stimulated for production. The water cut in the parent wells increased significantly due to the connection between the parent and child wells.

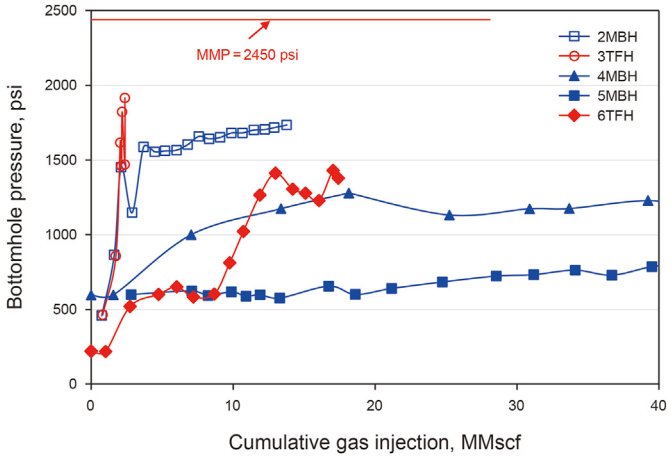

Fig. 4. Pressure response versus the cumulative gas injection volume for the five gas injection wells used in the pilot.

2019). Fig. 5a shows the injection rates and time in the two wells, while Fig. 5b shows the oil and gas production performance in Well 3TFH. Limited incremental oil production was observed in Well 3TFH when HnP operations were conducted in the well. The EOR effect reduced with cycles as indicated in Fig. 5b. For example, the change of oil production rate in 3TFH after the first cycle was from approximately 23 to 43 bpd, and after the second cycle, the oil production rate was from approximately 29 to 35 bpd. The incremental oil production effect did not last long in both cycles. Two cycles of HnP operations were also performed in Well 4MBH. The gas rate in Well 3TFH quickly responded to the HnP in Well 4MBH; however, the oil response in Well 3TFH was minimal, as shown in Fig. 5b. The quick gas breakthrough in Well 3TFH indicated that the two wells are connected, which made it difficult for pressure to build up around Well 4MBH, as shown in Fig. 4. Therefore, one of the conclusions from the pilot test was that conformance control is needed to raise the reservoir pressure and, thus, improve the EOR performance (Pospisil et al., 2020).

3. Simulation model development

The learnings from the field pilot test were used to test a set of synthetic cases using reservoir simulation. In order to investigate the operational strategies for EOR improvement, a fractured reservoir model was needed. The fracturing data for the simulated wells are shown in Table 2. Since simulating 16 full-scale wells with many fracture stages requires significant computational resources, 10%–12% of fracture stages for each well were included in the model. For example, Wells 4MBH and 2TFH have 50 and 35 fracture stages, respectively. However, in the fractured reservoir simulation model, five and four fracture stages were included in the model for Wells 4MBH and 2TFH, respectively. Flow simulation in fractured reservoirs is computationally challenging because of the large permeability contrast between the matrix and fractures. Therefore,

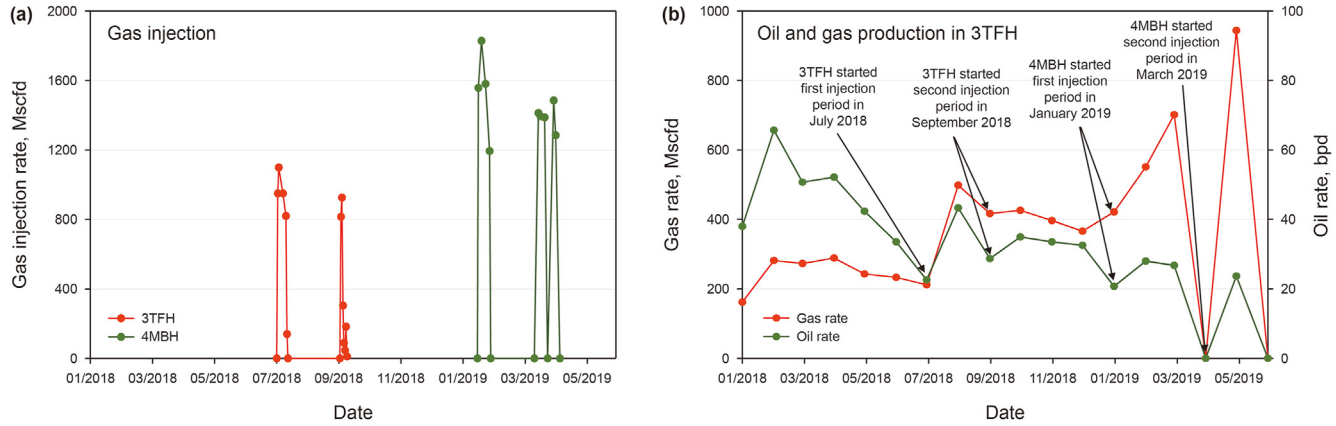

Fig. 5. Example of gas injection and oil production behavior in the pilot test: (**a**) gas injection rates in Wells 3TFH (Cycle 1: 07/03/18–7/14/18, Cycle 2: 09/03/18–09/10/18) and 4MBH (Cycle 1: 01/16/19–01/29/19, Cycle 2: 03/13/19–04/07/19); (**b**) oil and gas production in Well 3TFH. Note: the production data were reported in a monthly format, so the oil production rates were not zero in the months when gas was injected.

a high-efficiency fracture modeling method is needed to simulate the complex flow behavior in the studied reservoir, especially when gas is injected for EOR operations.

3.1. Embedded discrete fracture modeling

A few methods have been used for fractured reservoir simulation, including dual porosity and dual permeability method, local grid refinement method, unstructured grids, etc. (Warren and Root, 1963; Xu et al., 2017; Yu et al., 2014). However, these methods require long computational time when the fracture network becomes complex (Choi et al., 1997; Conlin et al., 1990; Mirzaei and Cipolla, 2012). A new fracture modeling method, EDFM, was developed recently to handle this challenge. The EDFM method employs a nonneighboring connection (NNC) approach to couple the matrix and fracture grids, which saves computational time significantly by reducing the noneffective fracture grids in the simulation model. Also, the NNC approach allows the simulation of three-dimensional nonplanar and slanted fractures using additional two-dimensional fracture cells. Therefore, the EDFM method can maintain simulation accuracy while significantly improving computational efficiency (Lee et al., 2001; Li and Lee, 2008; Moinfar et al., 2013; Wan, 2020; Wan et al., 2020; Xu, 2015; Xu et al., 2017). A detailed explanation of the EDFM method is shown in Fig. 6. The matrix block and fracture segments are shown in Fig. 6a, and corresponding cells are shown in Fig. 6b with the same color. Three types of NNCs are included in Fig. 6.

- NNC type I – matrix and fracture connection
- NNC type II – fracture segments connection in a single fracture
- NNC type III – the connection between two intersecting fracture segments

If a new fracture segment is added to the physical domain, then a nonneighboring new fracture cell will be added to the computational domain, accordingly, to calculate fluid flow inside fractures or between fractures and the rock matrix. Thus, the EDFM method allows complex fracture geometry to be simulated via structured grids. As a result, industry-standard reservoir simulators such as CMG's software package can be used to perform unconventional reservoir simulation efficiently using the fracture grids generated by EDFM (Xu, 2015; Xu et al., 2017).

3.2. Simulation model and history matching

In this study, the EDFM method was employed to create the fracture network, while CMG's compositional module, GEM, was utilized to perform the flow simulation. Based on the reservoir, well, and fracture data, a simulation model with both hydraulic and natural fractures was developed for the 16 wells in the EOR pilot. Literature suggests that the Bakken Formation is rich in natural fractures (Pitman et al., 2001). Thermal maturity evaluation, geomechanical properties (such as brittleness and stress anisotropy) measurement, and core sample analysis can be used to characterize and predict the occurrence of natural fractures (Kias et al., 2015; Mba and Prasad, 2010; Pitman et al., 2001). However, the field-scale natural fracture distribution to be used in the simulation model is uncertain. The fracture properties (such as fracture aperture, half-length, and permeability) and natural fracture distribution need to be tuned to ensure acceptable history matching performance (Liu, 2021; Liu et al., 2022; Wan et al., 2022).

Fig. 7 shows the distribution of wells and fractures in the model. The length (in the *Y* direction), width (in the *X* direction), and height (in the *Z* direction) of the model are 8000, 1000, and 840 ft, respectively. The model contains six intervals, including Lodgepole, UB, MB, LB, TF-1, and TF-2. The thicknesses of these intervals are 350, 10, 60, 30, 40, and 350 ft, respectively. The grid, porosity, and permeability information of the model are summarized in Table 3. History matching was performed to match the field production data by tuning the matrix and fracture parameters. Figs. 8 and 9 are example history-matching results for the field and Well 2MBH, respectively. Generally, the model matched the historical data reasonably well, indicating that the model can capture the flow dynamics between fractures and matrix in this site. Therefore, a series of EOR cases were designed to investigate the rich gas HnP performance considering the well interference in the reservoir.

History matching was performed to match the field production data by tuning the matrix and fracture parameters. Figs. 8 and 9 are example history-matching results for the field and Well 2MBH, respectively. Generally, the model matched the historical data reasonably well, indicating that the model can capture the flow dynamics between fractures and matrix in this site. Therefore, a series of EOR cases were designed to investigate the rich gas HnP performance considering the well interference in the reservoir.

4. Single-well huff 'n' puff EOR

Field data showed that the injected gas migrated to offset wells rapidly after injection started. This phenomenon was observed in all five gas injectors and their offset wells. Therefore, 22 cases were designed to capture the interwell flow behavior during single-well HnP, as shown in Table 4. The cases were developed to identify the minimum gas injection rate that is required to have a meaningful EOR response in the HnP well and whether water injection can

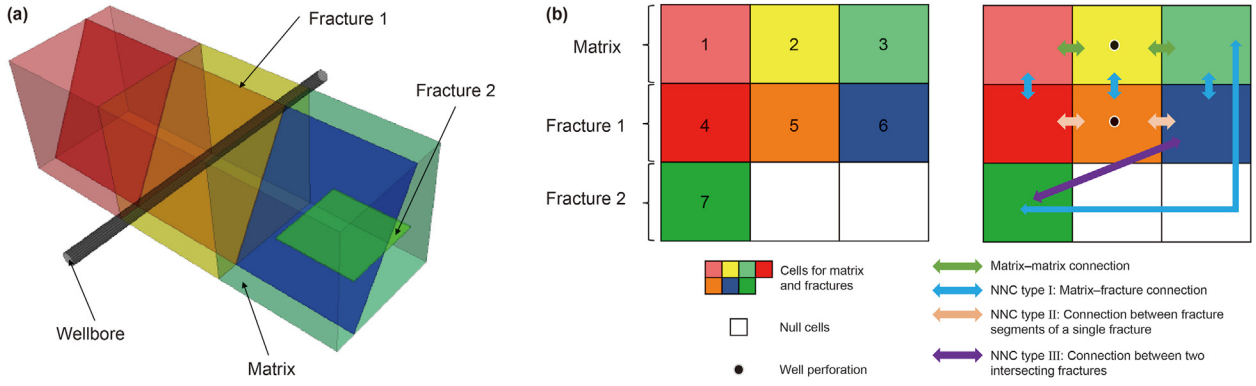

Fig. 6. Explanation of the (**a**) physical and (**b**) computational domains of EDFM and the connections between wellbore, fractures, and matrix (Xu et al., 2017; Jin et al., 2022a, 2022b).

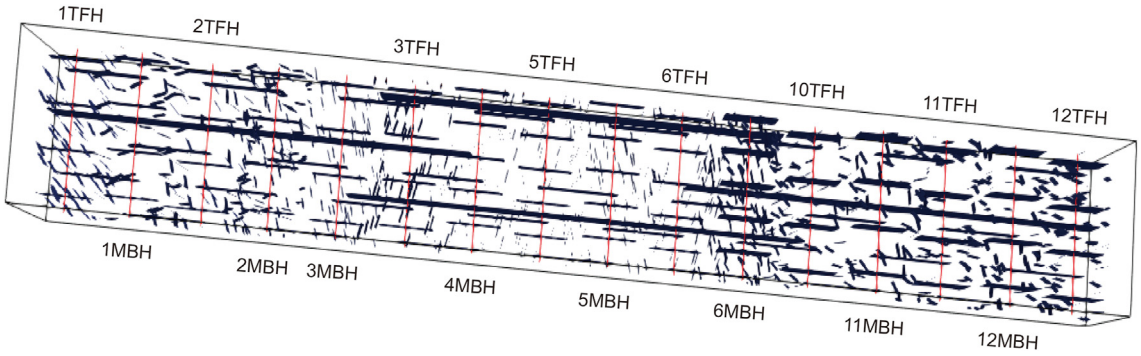

Fig. 7. Schematic of fracture distribution in the simulation model.

Table 3
Setup of the reservoir matrix in the simulation model.

	Formation	Number of cells	Cell size, ft	Permeability, mD	Porosity, fraction
X direction	–	10	100	–	–
Y direction	–	160	50	–	–
Z direction	Lodgepole	7	50	0.001	0.024
	UB	1	10	0.0004	0.054
	MB	3	20	0.00114	0.06
	LB	2	15	0.0003	0.07
	TF-1	3	10	0.00118	0.08
	TF-2	2	10	0.00145	0.09

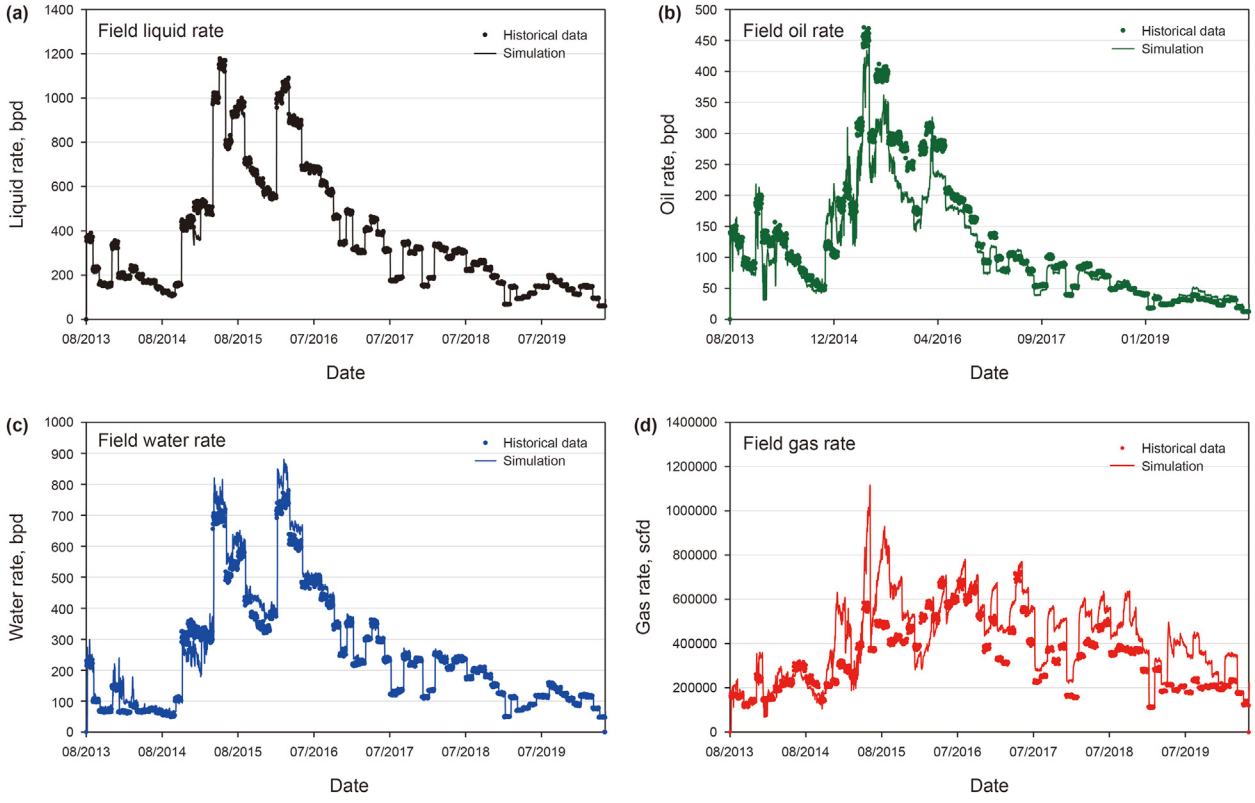

Fig. 8. History-match results for the field (sum of production for 16 wells): (**a**) liquid rate, (**b**) oil rate, (**c**) water rate, and (**d**) gas rate.

improve the EOR performance by controlling the conformance issues in the EOR processes. For the cases with variable gas injection rates from 3 to 20 MMscfd, the rates were set to 3, 6, 8, 10, 15, and 20 MMscfd. Table 5 shows the general parameters used in the single-well HnP cases. The injection time, soak time, and production time were set at 60, 0, and 30 days, respectively, for a total cycle

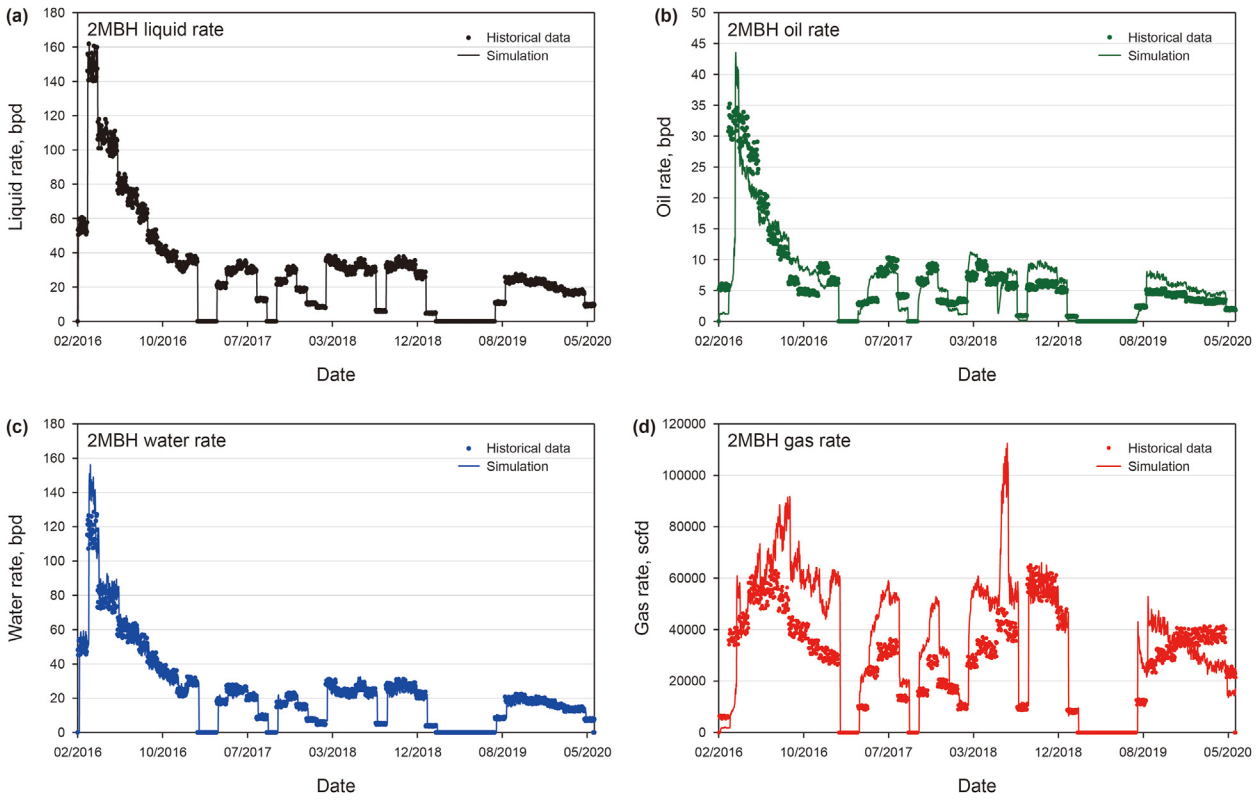

Fig. 9. History-match results for Well 2MBH: (**a**) liquid rate, (**b**) oil rate, (**c**) water rate, and (**d**) gas rate.

Table 4
Case design to test different scenarios for single-well HnP.

Testing effect	Case No.	HnP well	Gas injection rate, MMscfd	Offset well operations during the injection cycle
Injection rate	1–6	4MBH	3–20	Open
Injection rate	7–12	4MBH	3–20	Closed
Conformance control	13–17	2MBH	10	Open, closed, water injection
Conformance control	18–22	12MBH	10	Open, closed, water injection

time of 90 days per cycle.

4.1. Cases 1–6: Offset wells open during HnP

Cases 1 to 6 were designed to test the injection rate effect on EOR performance when the offset wells (3TFH and 5TFH) were open during the HnP process. The setup of the cases is shown in Table 6. Rich gas was injected through Well 4MBH during the injection stage, with an injection rate of 3, 6, 8, 10, 15, or 20 MMscfd. The well was open for production during the production stage. Because of the large, depleted volume in the reservoir, no soaking stage was used in these cases. Offset Wells 3TFH and 5TFH were open for production all the time.

Table 5
General parameters for all single-well HnP cases.

Parameter	Value
EOR operational time	2 years
Injection time	60 days/cycle
Soaking time	0 days/cycle
Production time	30 days/cycle
Injection gas composition (C_1: C_2: C_3)	7:2:1
Maximum gas injection pressure constraint	7500 psi
Minimum production pressure constraint	300 psi

Table 6
Settings for the HnP and offset wells of Cases 1 to 6.

Case No.	HnP well		Offset well	
	Name	Injection rate, MMscfd	Name	Operation
1	4MBH	3	3TFH, 5TFH	Open
2	4MBH	6	3TFH, 5TFH	Open
3	4MBH	8	3TFH, 5TFH	Open
4	4MBH	10	3TFH, 5TFH	Open
5	4MBH	15	3TFH, 5TFH	Open
6	4MBH	20	3TFH, 5TFH	Open

Fig. 10 shows the effect of gas injection rate on EOR performance of 4MBH when offset wells were open. The simulation results suggested that a higher gas injection rate contributed to higher cumulative oil production. The results also suggested that a gas injection rate lower than 10 MMscfd could not improve oil production in the HnP well, as these cases all plotted below the pressure depletion case. Fig. 11 shows the distribution of gas saturation in the fractures after the first injection stage of Cases 1, 4, and 6 (with the gas injection rates of 3, 10, and 20 MMscfd, respectively). Fig. 11 indicates that the injected gas was not distributed evenly in each fracture around the HnP well; gas could flow to offset wells

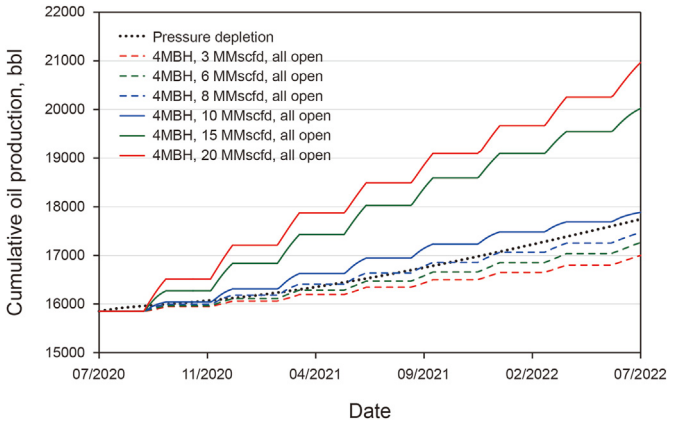

Fig. 10. Effect of gas injection rate on EOR performance of a single-well HnP when offset wells were open. The black dotted line represents the base case with no HnP EOR and, therefore, the reference against which to compare the EOR cases.

without fully filling up the fractures when the gas injection rate was less than or equal to 10 MMscfd. Fig. 12 shows the pressure distribution in the fractures for the same cases. Like the gas saturation distribution, the pressure distribution in the fractures was uneven, especially when the gas injection rate was below 10 MMscfd. However, both gas saturation and pressure distribution profiles changed when the gas injection rate reached 20 MMscfd, as shown in Figs. 11c–12c, respectively, where the highest gas saturation and pressure were observed in the fractures around the HnP well. Gas filled up most of the hydraulic fractures around the well and raised the pressure to 6000 psi at the end of the first injection stage. Therefore, the injected gas could penetrate the tight matrix and interact with oil within the fractures for EOR. As a result, an effective EOR response was observed when the gas injection rate was high enough, as illustrated in Fig. 10.

4.2. Cases 7–12: Offset wells closed during injection

Since all offset wells were open in the HnP process of Cases 1–6, the injected gas migrated to offset wells through the interconnected fractures at the end of 2 years of HnP operations, as shown in Fig. 13. Cases 7 to 12 were designed to investigate whether closing the offset wells in the injection process could reduce the crossflow between the HnP and offset wells and, thereby, improve production performance. Table 7 shows the basic parameter settings for these cases. 4MBH was the HnP well; the offset wells (3TFH and 5TFH) were closed during the injection stage and open to production during the production stage. Other wells were open to production during the entire 2 years of operations. Fig. 14a shows the oil production performance of Cases 7 to 12. Generally, the EOR trend of Cases 7–12 was comparable to that of Cases 1–6, as shown in Fig. 14b. The comparison showed that closing the offset wells could be beneficial to improving the cumulative oil production in the HnP wells when the injection rates were 10 and 15 MMscfd; however, the improvement was not significant. The results of Cases 1–12 indicated that closing offset wells was not a sufficient operating strategy for reducing interwell gas flow and improving EOR performance. Therefore, additional cases were investigated to explore whether conformance control could improve the EOR performance.

4.3. Improvement of single-well HnP EOR

Since the 16 wells in the pilot area have different production and completion histories, as shown in Tables 1 and 2, respectively, the HnP EOR performance for each well could also be different. To cover more wells in this study, different wells were selected to investigate the EOR performance with and without conformance control. An

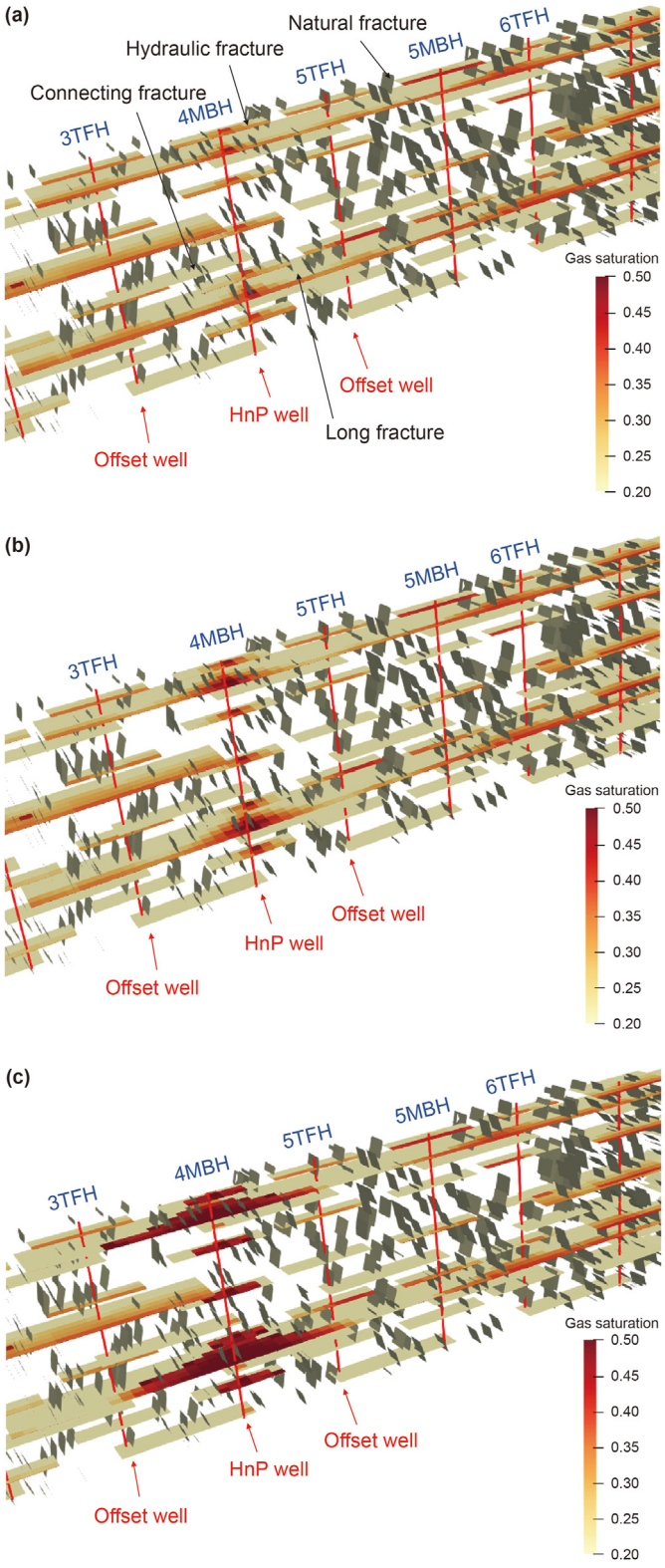

Fig. 11. Gas saturation distribution after the first cycle of injection in Cases 1, 4, and 6, with the gas injection rates of (**a**) 3 MMscfd, (**b**) 10 MMscfd, and (**c**) 20 MMscfd.

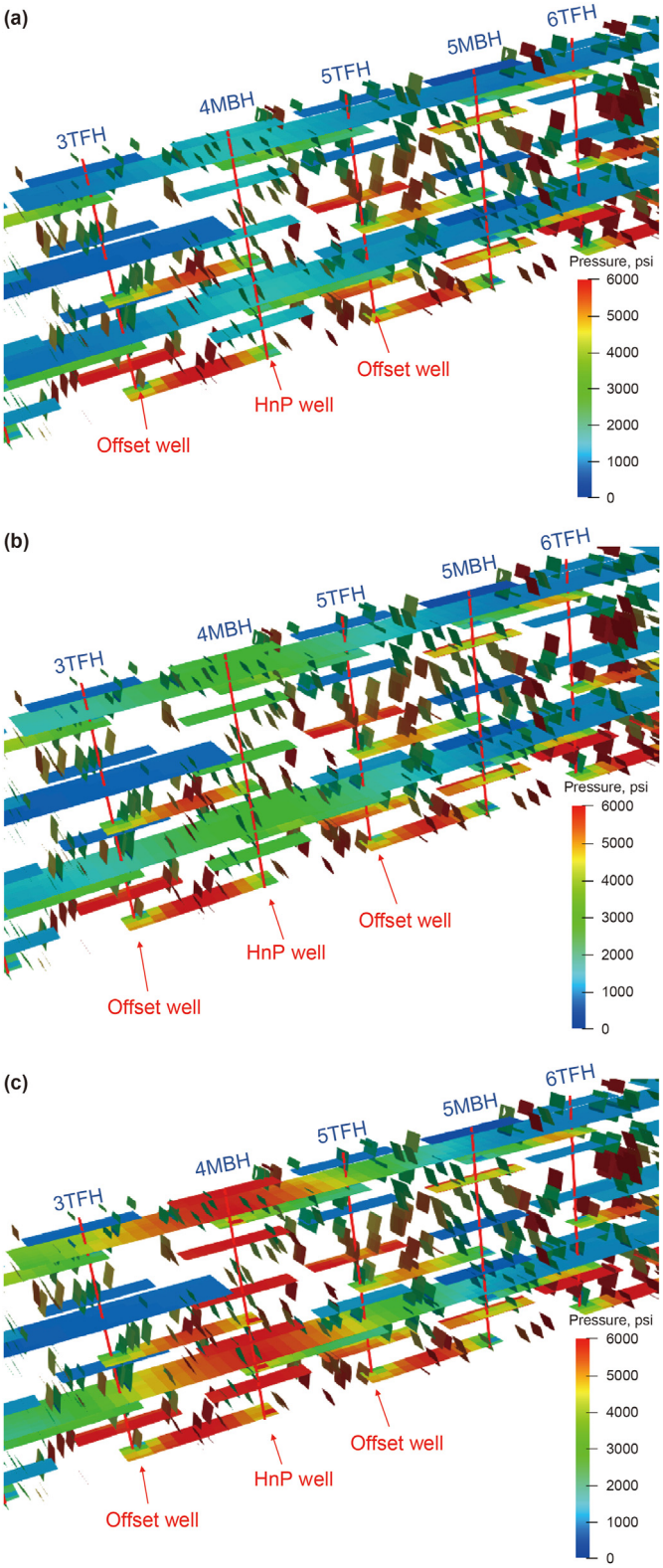

Fig. 12. Pressure distribution in fractures after the first injection stage of Cases 1, 4, and 6, with the gas injection rates of (**a**) 3 MMscfd, (**b**) 10 MMscfd, and (**c**) 20 MMscfd.

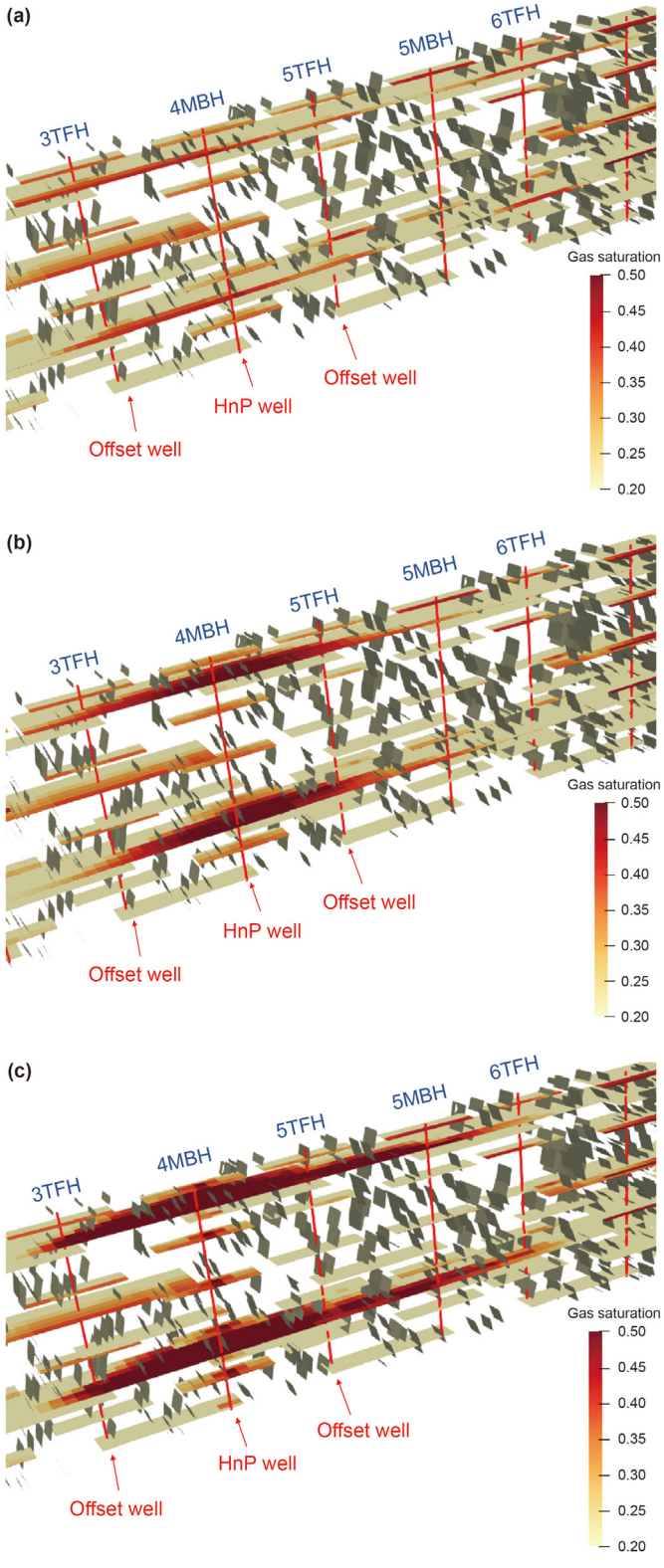

Fig. 13. Gas saturation distribution after 2 years of HnP for Cases 1, 4, and 6, with the gas injection rates of (**a**) 3 MMscfd, (**b**) 10 MMscfd, and (**c**) 20 MMscfd.

additional ten cases (Cases 13–22) were designed to compare the EOR results of the HnP wells when their offset wells were open, closed, and injecting water for conformance control. The detailed settings for these cases can be found in Table 8.

Fig. 15a shows the cumulative oil production of Cases 13–17 when Well 2MBH was used for HnP operations for 2 years. The curves indicate that the conformance control with water injection in the offset wells (2TFH and 3MBH) could significantly improve the

Table 7
Setup parameters for the HnP and offset wells of Cases 7 to 12.

Case No.	HnP well		Offset well	
	Name	Injection rate, MMscfd	Name	Operation
7	4MBH	3	3TFH, 5TFH	Closed
8	4MBH	6	3TFH, 5TFH	Closed
9	4MBH	8	3TFH, 5TFH	Closed
10	4MBH	10	3TFH, 5TFH	Closed
11	4MBH	15	3TFH, 5TFH	Closed
12	4MBH	20	3TFH, 5TFH	Closed

EOR performance in Well 2MBH—the cumulative oil production during the 2-year EOR process of Case 17 (3671 bbl) was 2.7 times more than that of Case 13 (1370 bbl) because water was injected at 6000 psi in the offset wells in Case 17. The same EOR response was observed in Well 12MBH, as shown in Fig. 15b.

The cases with water injection showed that higher water injection pressure in the offset wells led to more oil production in the HnP well. Since gas flows from the HnP well to its offset wells during the injection stage because of the pressure differential between the HnP and offset wells, injecting water in the offset wells

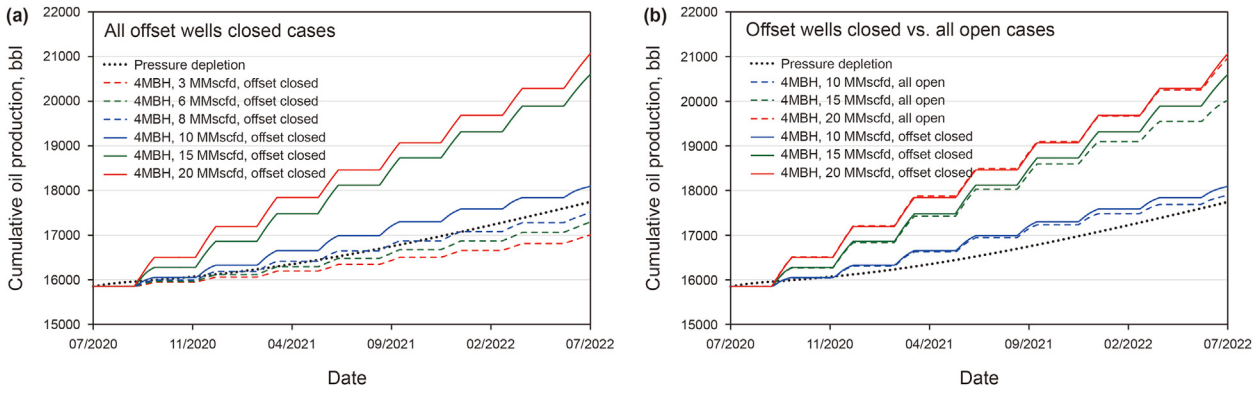

Fig. 14. Effect of gas injection rate on cumulative oil production of the HnP well for (**a**) all offset wells closed Cases 7 to 12 and (**b**) comparison of EOR performance with open and close of offset wells. The black dotted line represents the base case with no HnP EOR and, therefore, the reference against which to compare the EOR cases.

Table 8
Setup parameters for the HnP and offset wells of Cases 13 to 22.

Case No.	HnP well		Offset well		
	Name	Injection rate, MMscfd	Name	Operation	Water injection pressure, psi
13	2MBH	10	2TFH, 3MBH	Open	–
14	2MBH	10	2TFH, 3MBH	Closed	–
15	2MBH	10	2TFH, 3MBH	Water injection	2000
16	2MBH	10	2TFH, 3MBH	Water injection	4000
17	2MBH	10	2TFH, 3MBH	Water injection	6000
18	12MBH	10	11TFH, 12TFH	Open	–
19	12MBH	10	11TFH, 12TFH	Closed	–
20	12MBH	10	11TFH, 12TFH	Water injection	2000
21	12MBH	10	11TFH, 12TFH	Water injection	4000
22	12MBH	10	11TFH, 12TFH	Water injection	6000

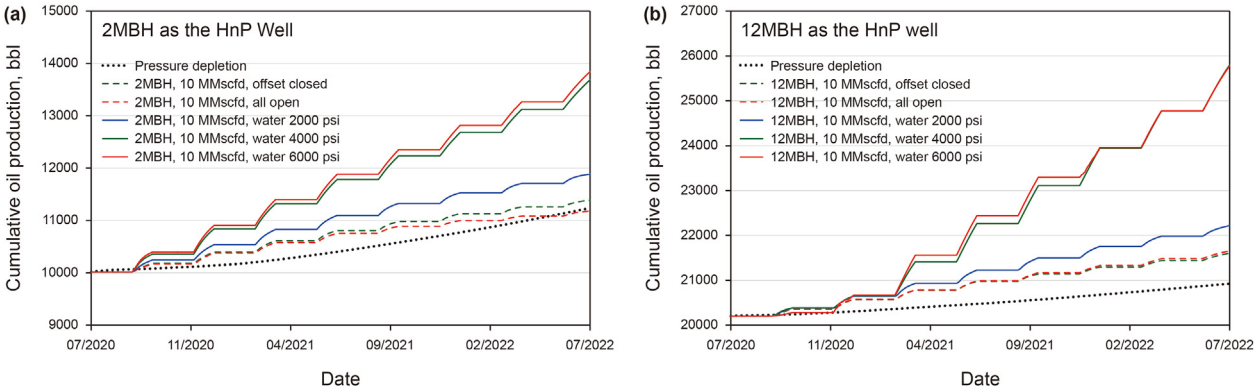

Fig. 15. HnP well cumulative oil production curves for (**a**) Cases 13 to 17, with 2MBH as the HnP well, and (**b**) Cases 18 to 22, with 12MBH as the HnP well, when different operations were performed in their offset wells. The black dotted line represents the base case with no HnP EOR and, therefore, the reference against which to compare the EOR cases.

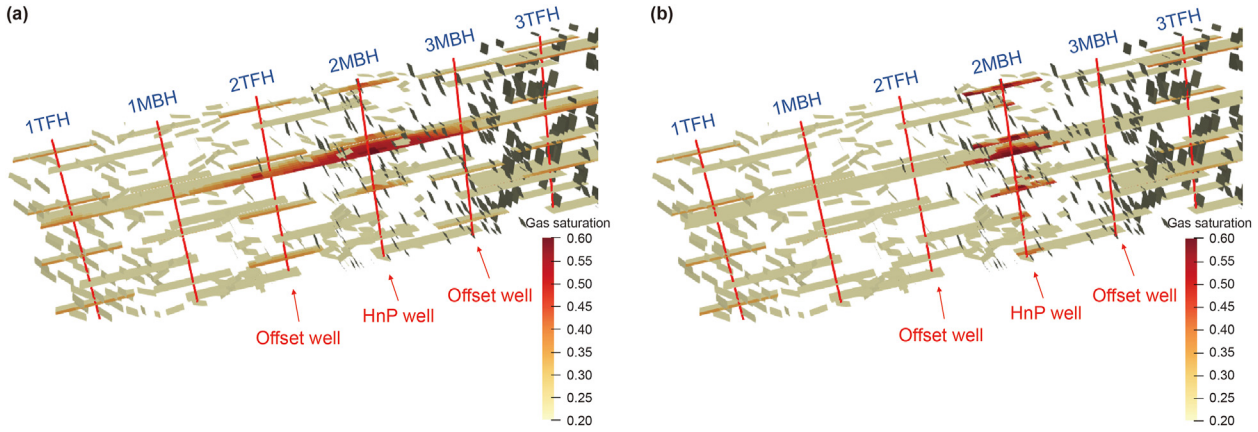

Fig. 16. Gas saturation distribution around Well 2MBH after the last cycle of injection in (**a**) Case 13 (no conformance control and offset wells open) and (**b**) Case 17 (with water injection conformance control in the offset wells).

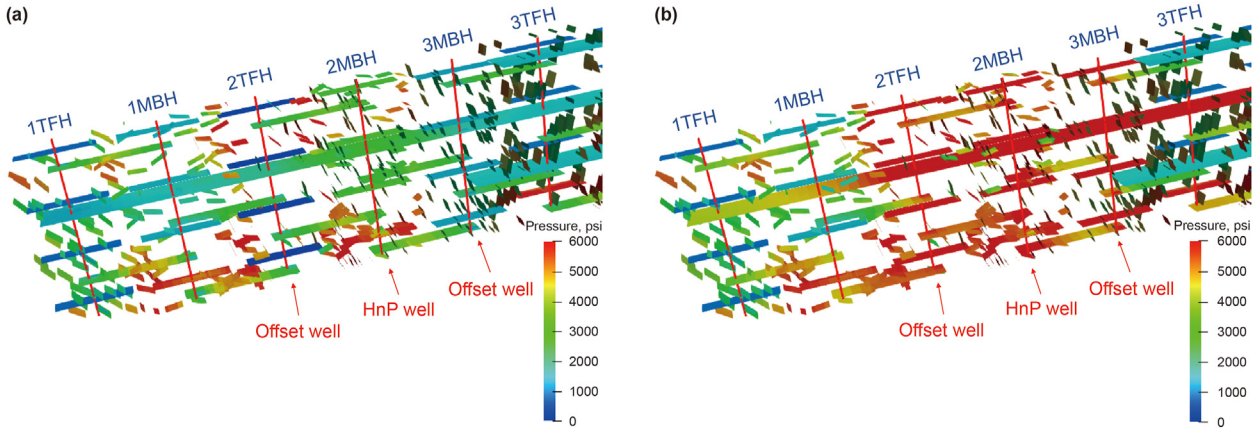

Fig. 17. Pressure distribution around Well 2MBH after the last cycle of injection in (**a**) Case 13 (no conformance control and offset wells open) and (**b**) Case 17 (with water injection conformance control in the offset wells).

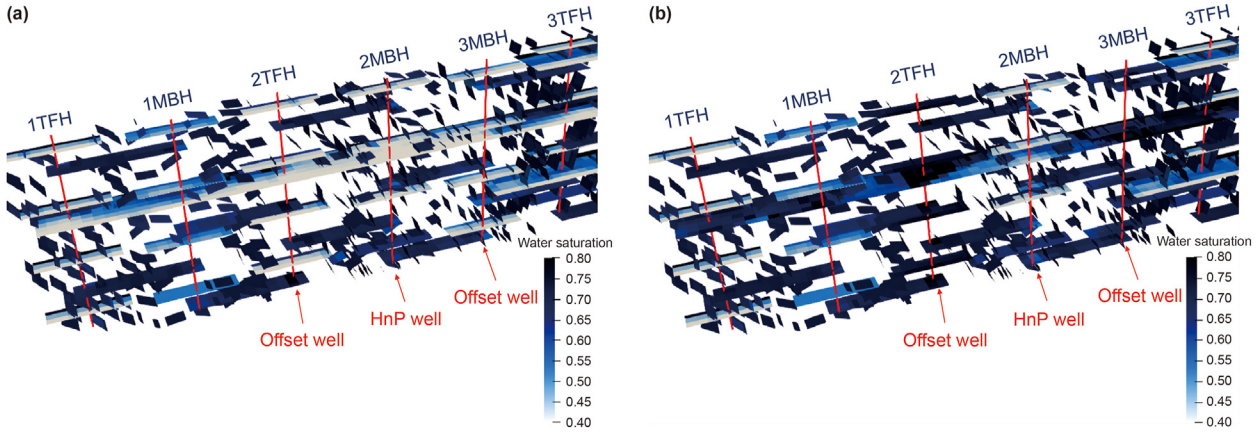

Fig. 18. Water saturation distribution around Well 2MBH after the last cycle of injection in (**a**) Case 13 (no conformance control and offset wells open) and (**b**) Case 17 (with water injection conformance control in the offset wells).

can prevent undesired gas flow by raising the pressure around the offset wells. As a result, the injected gas could be maintained around the HnP well for lifting pressure there. Figs. 16–18 show the gas saturation, pressure, and water saturation distribution profiles around Well 2MBH with and without water injection in its offset wells, respectively. The figures clearly illustrate the effect of conformance control on increasing the gas saturation and pressure around the HnP well: gas migrated to the offset wells through the high-permeability fractures when the offset wells were open during the injection stage (Fig. 16a); however, this issue was effectively

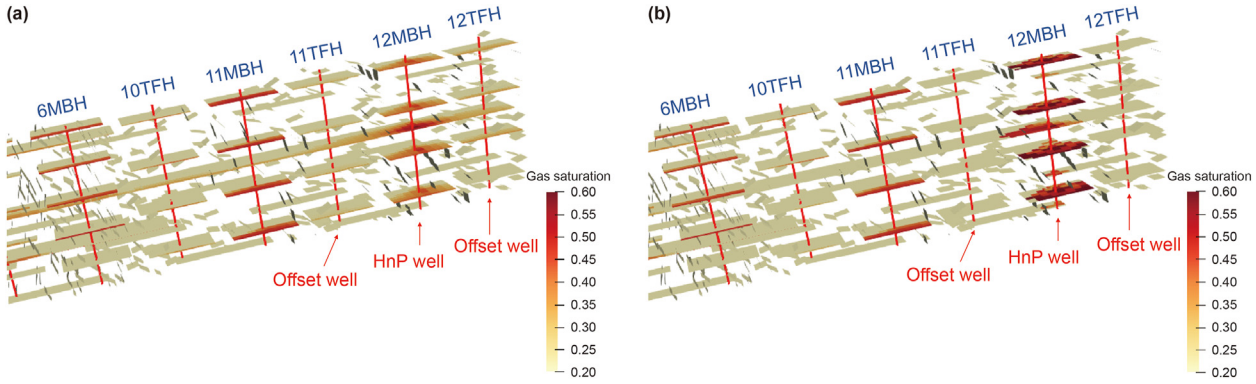

Fig. 19. Gas saturation distribution around Well 12MBH after the last cycle of injection in (**a**) Case 18 (no conformance control and offset wells open) and (**b**) Case 22 (with water injection conformance control in the offset wells).

controlled by water injection in the offset wells so that the injected gas can fill the hydraulic fractures more evenly around the HnP well (Fig. 16b). With water injected into the offset wells, water filled the hydraulic fractures and the long fracture around the offset wells, but did not fill the fractures around the HnP well (Fig. 18b). Similar phenomena were observed around Well 12MBH, as shown in Figs. 19–21. The results confirmed that proper pressure containment allows injection gas to penetrate the reservoir matrix via hydraulic and connecting fractures, thus a larger volume of reservoir can be accessed for EOR purposes.

5. Multiple-well EOR strategies

Figs. 14 and 15 show that the EOR response to gas injection varies widely from well to well. For example, Well 12MBH requires less gas injection than Wells 4MBH and 2MBH to yield positive EOR results. Although water injection in the offset wells can improve the EOR performance in the HnP well by confining the gas around the HnP well, oil production in the offset wells may be reduced since water injection leads to higher water saturation around the offset wells. Because oil and water are immiscible, the high interfacial tension between the two phases and the tiny pore throat size in the

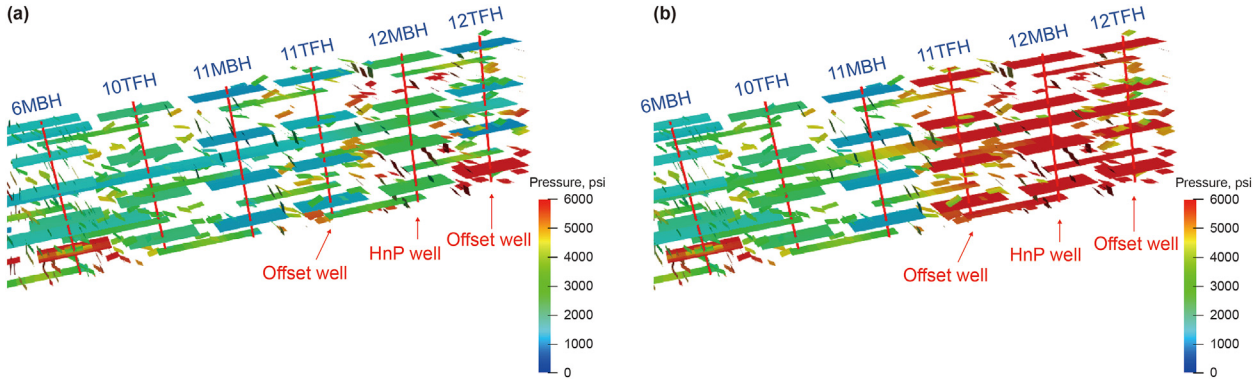

Fig. 20. Pressure distribution around Well 12MBH after the last cycle of injection in (**a**) Case 18 (no conformance control and offset wells open) and (**b**) Case 22 (with water injection conformance control in the offset wells).

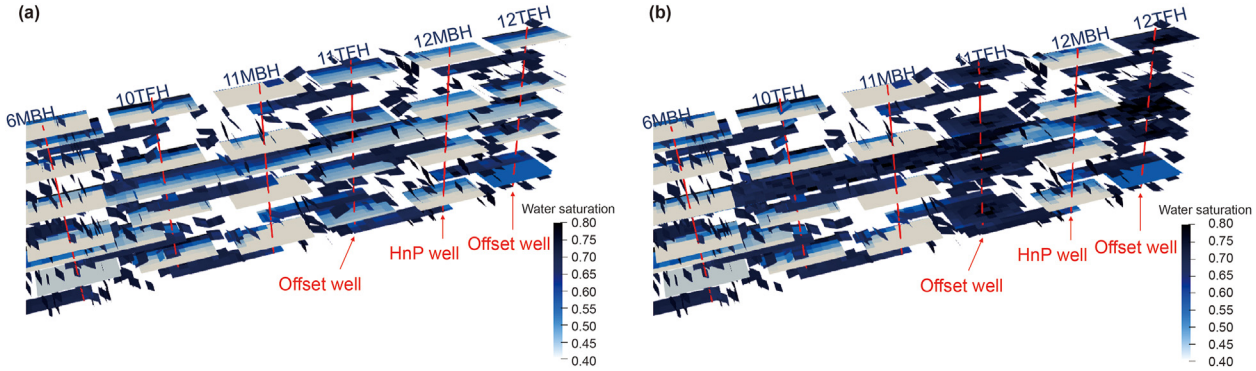

Fig. 21. Water saturation distribution around Well 12MBH after the last cycle of injection in (**a**) Case 18 (no conformance control and offset wells open) and (**b**) Case 22 (with water injection conformance control in the offset wells).

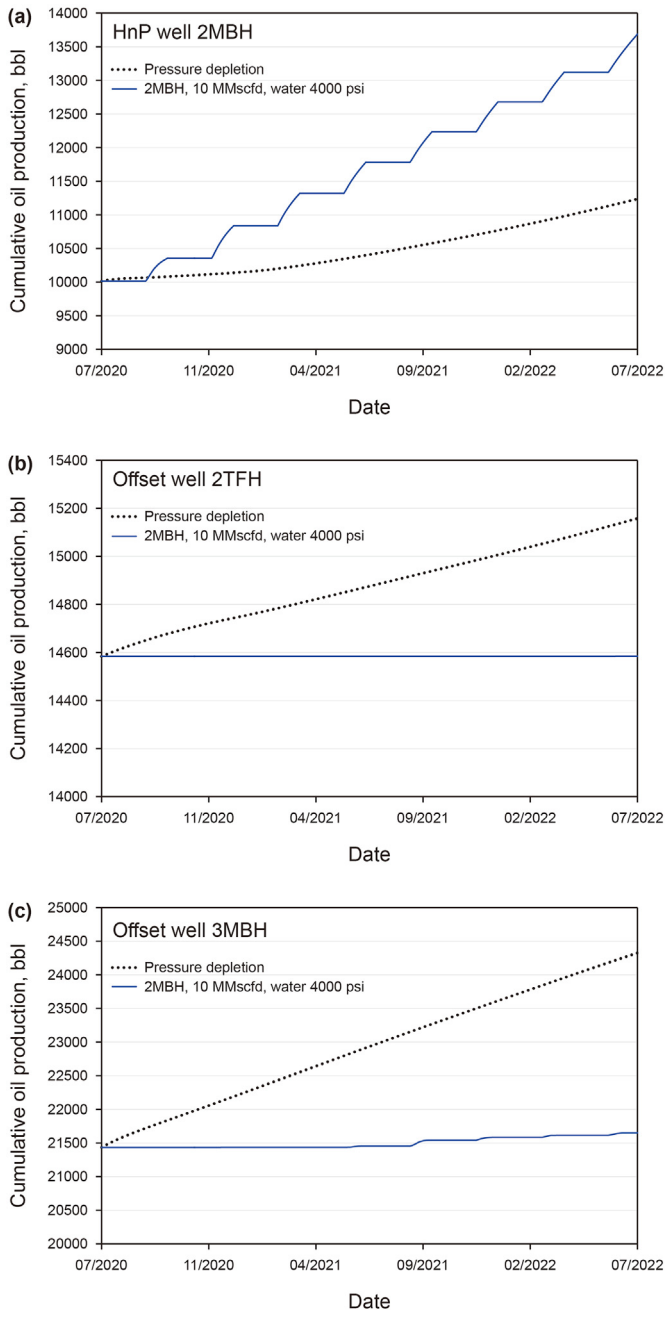

Fig. 22. Oil production performance in different wells for Case 16: (**a**) HnP Well 2MBH, (**b**) offset Well 2TFH, and (**c**) offset Well 3MBH. The black dotted line represents the base case with no HnP EOR and, therefore, the reference against which to compare the EOR cases.

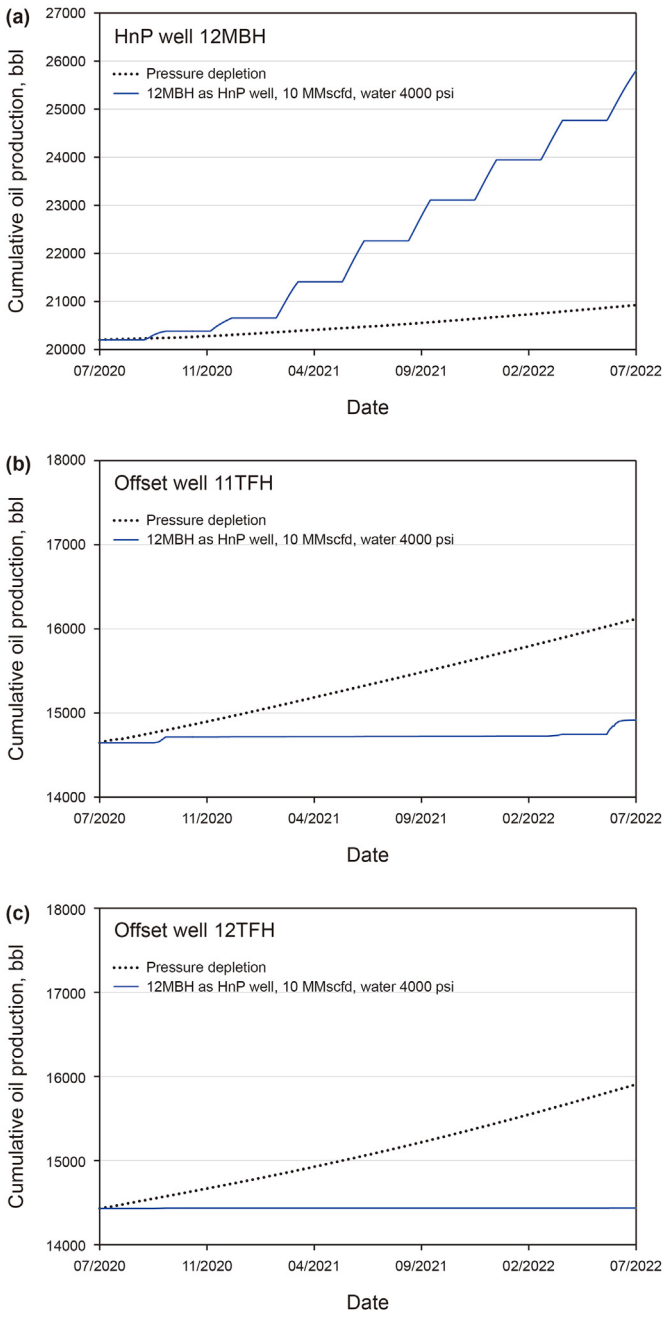

Fig. 23. Oil production performance in different wells for Case 21: (**a**) HnP Well 12MBH, (**b**) offset Well 11TFH, and (**c**) offset Well 12TFH. The black dotted line represents the base case with no HnP EOR and, therefore, the reference against which to compare the EOR cases.

rock lead to high capillary pressure in the reservoir, which could block oil flowing from the matrix to fractures.

Fig. 22 compares the oil production in 2MBH and two offset wells (2TFH and 3MBH) for Case 16, where water was injected into the offset wells at a constant pressure of 4000 psi. Although oil production was improved in the HnP well (Fig. 22a), the two offset wells lost most of their production because of the lost production time during the injection phase of each cycle (60 days per cycle, or 120 total during the 2-year EOR period) (Fig. 22b and c). The net increase in production for the HnP Well 2MBH was 2451 bbl, but the net loss in production for Offset Well 2TFH (−573 bbl) and Well 3MBH (−2676 bbl) was −3249 bbl total, for a net loss of production of −798 bbl for the three wells (sum of 2MBH, 2TFH, and 3MBH). Therefore, the positive effect of water injection on oil production in the HnP well could not compensate for the loss of oil production in the offset wells in this case. For Case 21, the situation changed, as shown in Fig. 23, where the incremental oil in the HnP well (12MBH, 4877 bbl) was more than the loss of oil production in the offset wells (11TFH [−1202 bbl] and 12TFH [−1468 bbl]). The results indicated that the wells need to be considered individually when designing EOR strategies to optimize the overall EOR performance for the entire pilot site.

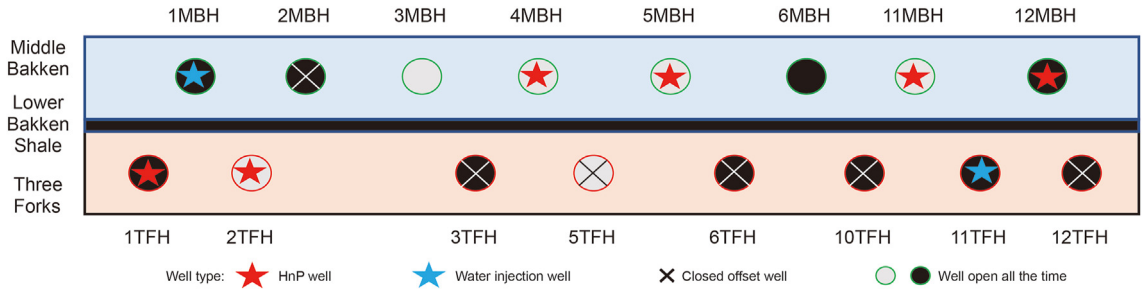

Fig. 24. Distribution of different types of wells in the EOR site.

Table 9
General parameters for multiple-well HnP EOR.

Parameter	Value
EOR operational time	2 years
Injection time	30 days/cycle
Soaking time	0 days/cycle
Production time	60 days/cycle
Injection gas composition (C_1: C_2: C_3)	7:2:1
Maximum gas injection pressure constraint	7500 psi
Minimum production pressure constraint	300 psi

After analyzing the oil production performance for all 16 wells individually, an additional set of cases was simulated to assess EOR performance for a broader set of wells. Six wells (1TFH, 2TFH, 4MBH, 5MBH, 11MBH, and 12MBH) were selected as HnP wells, two wells (1MBH and 11TFH) were selected as water injectors for conformance control, six wells (2MBH, 3TFH, 5TFH, 6TFH, 10TFH, and 12TFH) were closed during the injection stage and then open in the production stage of the HnP process, and two wells (3MBH and 6MBH) remained open all the time. Fig. 24 shows the distribution of these wells in the site. Four cases were designed to investigate the overall EOR performance in the site, considering conformance control with water injection (Cases 23–26). The detailed parameter settings can be found in Tables 9 and 10. Since six wells were used for gas HnP operations and two wells were water injectors for conformance control, more injected gas could flow through fractures into the matrix than the single well HnP cases during the same injection time. Shorter injection time and longer production time could minimize the detrimental effect of water breakthrough and allow oil to be produced for a longer time. The gas injection and oil production time were set to 30 and 60 days/cycle, respectively. The maximum gas injection rate was set at 10 MMscfd for each HnP well. The water injection wells (1MBH and 11 TFH) were set as regular producers and were closed when gas was injected during the EOR process in Case 23. Water was injected at different pressures in Cases 24–26 to test the effect of conformance control on overall EOR performance. Fig. 25 shows the comparison of the overall EOR performance in the site for Cases 23–26. The results are summarized in Table 11. The results indicated that the case of no

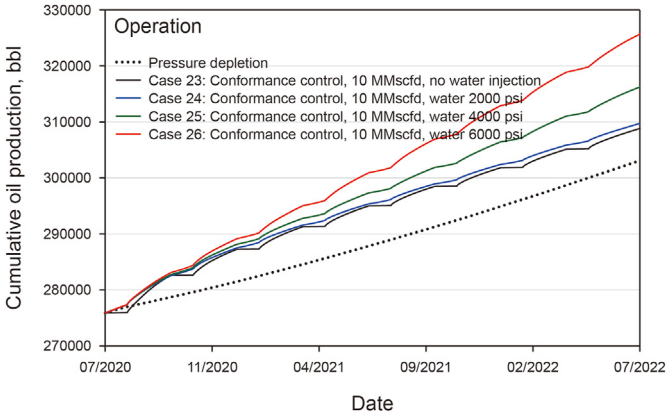

Fig. 25. Comparison of cumulative oil production in the pilot site (sum of production for 16 wells) for Cases 23 to 26. The black dotted line represents the base case with no HnP EOR and, therefore, the reference against which to compare the EOR cases.

water injection (Case 23) could improve oil production by 1.9% (303,107 bbl with no conformance control to 308,830 bbl with offset wells closed), while the case with water injection at 6000 psi (Case 26) could yield 7.4% of incremental oil production in 2 years of EOR operations (303,107 bbl with no conformance control to 325,657 bbl with water injection conformance control).

Both experimental and field results showed that propane can significantly reduce the pressure required to have effective interactions between oil and gas under the Bakken reservoir conditions (pressure of 6800 to more than 8000 psi, temperature of 220–260 °F, and oil gravity of 38–44 °API) (Hawthorne et al., 2020, 2021; Litvak et al., 2020; Nagarajan et al., 2020; Ozowe et al., 2020). Therefore, Case 27 was designed using the same operational settings as Case 26 but with propane as the injection gas to evaluate the effect of injection gas composition on EOR performance. In Case 27, all parameters were set the same as Case 26 except the injection gas composition, which was changed from rich gas to pure propane. Fig. 26 shows the comparison of cumulative oil production among different cases: pressure depletion (no EOR), rich gas EOR, and propane EOR. Results showed that using propane as an injection

Table 10
Well settings in Cases 23 to 26.

Case No.	HnP well		Offset well	
	Name	Injection rate, MMscfd/well	Type	Water injection pressure, psi
23	6 wells$^+$	10	Closed	–
24	6 wells$^+$	10	Water injection	2000
25	6 wells$^+$	10	Water injection	4000
26	6 wells$^+$	10	Water injection	6000

Note: $^+$six wells include 1TFH, 2TFH, 4MBH, 5MBH, 11MBH, and 12MBH.

Table 11
Well settings in Cases 23 to 27.

Case	Description	Oil production, bbl	Incremental oil, bbl	Percent change from base case, %
Base case	Pressure depletion	303,107	–	–
23	No water injection with rich gas	308,830	5723	1.9
24	2000 psi with rich gas	309,740	6633	2.2
25	4000 psi with rich gas	316,222	13,115	4.3
26	6000 psi with rich gas	325,657	22,550	7.4
27	6000 psi with propane gas	344,180	41,073	14.0

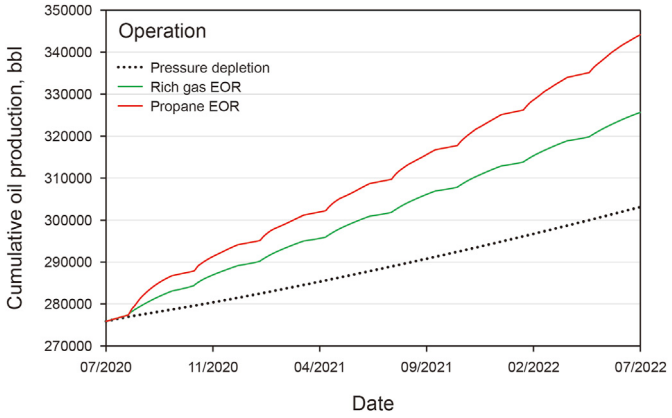

Fig. 26. Comparison of cumulative oil production among different cases: pressure depletion, rich gas EOR, and propane EOR. The black dotted line represents the base case with no HnP EOR and, therefore, the reference against which to compare the EOR cases.

gas could improve oil production by as much as 14% compared to pressure depletion for the site with 16 wells, and by as much as 5.7% compared to the rich gas EOR scenario.

6. Conclusions and recommendations

A series of field data analyses and simulation activities have been conducted to investigate strategies to improve oil production performance in a site with 16 wells in the Bakken unconventional play. A multiple-well, multiple-fracture simulation model was developed using the EDFM technology. The high efficiency of this fracture simulation method made it possible to identify the optimal EOR strategies with conformance control considered. Twenty-seven cases were designed to investigate the EOR performance of both single wells and the entire site. The following conclusions were obtained based on the results of this study.

(1) A minimum rich gas injection rate of 10 MMscfd was required to yield meaningful incremental oil production in both single- and multiple-well EOR processes in the studied site.
(2) Conformance control plays an important role in the gas HnP EOR process. Water injection in the offset wells could control conformance issues and improve oil production in the HnP well, but could also reduce the oil production in the offset wells. A proper conformance control design ensures that the oil production gain in the HnP well could compensate for the oil production loss in the offset wells.
(3) Different wells have different EOR responses to gas HnP operations, even in the same pilot site. A reasonable arrangement was required to optimize the EOR performance in a site with many wells. Rich gas HnP could improve cumulative oil production by 7.4% in the studied area.
(4) Replacing rich gas with propane as the injection gas could result in 14% of incremental oil production in the pilot site when conformance control was employed.

The learnings from this work can be leveraged for future applications of gas injection HnP with conformance control in the Bakken and other unconventional reservoirs. In this study, one set of matrix and fracture properties was utilized to obtain a history matching solution. Future work can focus on the better characterization of fractures in the reservoir. Image logging is recommended to be applied for multiple wells in the field to better characterize fracture distribution and interwell fracture connection. Multiple history matching solutions with different matrix and fracture properties setups are recommended to be obtained to address the uncertainty of fractures in the reservoir. Another direction of future work is investigating other EOR strategies such as gas and foam EOR. Adding foam can also correct the conformance issue and improve the sweep efficiency of gas floods. However, the foam needs to be carefully designed to be successfully applied to the high salinity and high temperature conditions of the Bakken.

Disclaimers

U.S. Department of Energy

This work was prepared as an account of work sponsored by an agency of the United States Government. Neither the United States Government, nor any agency thereof, nor any of their employees, makes any warranty, express or implied, or assumes any legal liability or responsibility for the accuracy, completeness, or usefulness of any information, apparatus, product, or process disclosed, or represents that its use would not infringe privately owned rights. Reference herein to any specific commercial product, process, or service by trade name, trademark, manufacturer, or otherwise does not necessarily constitute or imply its endorsement, recommendation, or favoring by the United States Government or any agency thereof. The views and opinions of authors expressed herein do not necessarily state or reflect those of the United States Government or any agency thereof.

North Dakota Industrial Commission

This work was prepared by the Energy & Environmental Research Center (EERC) pursuant to an agreement partially funded by the Industrial Commission of North Dakota, and neither the EERC nor any of its subcontractors nor the North Dakota Industrial Commission nor any person acting on behalf of either:

(A) Makes any warranty or representation, express or implied, with respect to the accuracy, completeness, or usefulness of the information contained in this report or that the use of any information, apparatus, method, or process disclosed in this report may not infringe privately owned rights; or

(B) Assumes any liabilities with respect to the use of, or for damages resulting from the use of, any information, apparatus, method, or process disclosed in this report.

Reference herein to any specific commercial product, process, or service by trade name, trademark, manufacturer, or otherwise does

not necessarily constitute or imply its endorsement, recommendation, or favoring by the North Dakota Industrial Commission. The views and opinions of authors expressed herein do not necessarily state or reflect those of the North Dakota Industrial Commission.

Declaration of competing interest

The authors declare that they have no known competing financial interests or personal relationships that could have appeared to influence the work reported in this paper.

Acknowledgments

This work is supported by the U.S. Department of Energy National Energy Technology Laboratory under Award No. DE-FE0024233 and the North Dakota Industrial Commission under the Award Nos. G-04-080 (BPOP 2.0) and G-051-98 (BPOP 3.0). The modeling work conducted under this program was made possible by the contributions of software licenses from CMG, SimTech, and Schlumberger.

References

Alvarado, V., Manrique, E., 2010. Enhanced oil recovery—an update review. Energies 3 (9), 1529–1575. https://doi.org/10.3390/en3091529.

Barajas-Olalde, C., Mur, A., Adams, D.C., Jin, L., He, J., Hamling, J.A., Gorecki, C.D., 2021. Joint impedance and facies inversion of time-lapse seismic data for improving monitoring of CO_2 incidentally stored from CO_2 EOR. Int. J. Greenh. Gas Control 112, 103501. https://doi.org/10.1016/j.ijggc.2021.103501.

Burrows, L.C., Haeri, F., Cvetic, P., Sanguinito, S., Shi, F., Tapriyal, D., Goodman, A., Enick, R.M., 2020. A literature review of CO_2, natural gas, and water-based fluids for enhanced oil recovery in unconventional reservoirs. Energy Fuels 34, 5331–5380. https://doi.org/10.1021/acs.energyfuels.9b03658, 2020.

Castro-Alvarez, F., Marsters, P., Ponce de León Barido, D., Kammen, D.M., 2018. Sustainability lessons from shale development in the United States for Mexico and other emerging unconventional oil and gas developers. Renew. Sustain. Energy Rev. 82, 1320–1332. https://doi.org/10.1016/j.rser.2017.08.082.

Choi, E.S., Cheema, T., Islam, M.R., 1997. A new dual-porosity/dual-permeability model with non-Darcian flow through fractures. J. Petrol. Sci. Eng. 17 (3–4), 331–344. https://doi.org/10.1016/S0920-4105(96)00050-2.

Conlin, J.M., Hale, J.L., Sabathier, J.C., Faure, F., Mas, D., 1990. Multiple-fracture horizontal wells—performance and numerical simulation. In: European Petroleum Conference. https://doi.org/10.2118/20960-MS.

Energy Information Administration, 2021. Drilling productivity report. https://www.eia.gov/petroleum/drilling/. February 2022.

Ganjdanesh, R., Eltahan, E., Sepehrnoori, K., Drozd, H., Ambrose, R., 2020. A field pilot of huff-n-puff gas injection for enhanced oil recovery in Permian Basin. In: SPE Annual Technical Conference and Exhibition. https://doi.org/10.2118/201622-MS.

Gaswirth, S.B., Marra, K.R., 2014. U.S. Geological survey 2013 assessment of undiscovered resources in the Bakken and Three Forks Formations of the U.S. Williston Basin Province. AAPG (Am. Assoc. Pet. Geol.) Bull. 99 (4), 639–660. https://doi.org/10.3133/fs20133013.

Hawthorne, S.B., Miller, D.J., Jin, L., Gorecki, C.D., 2016. Rapid and simple capillary-rise/vanishing interfacial tension method to determine crude oil minimum miscibility pressure—pure and mixed CO_2, methane, and ethane. Energy Fuel. 30 (8), 6365–6372. https://doi.org/10.1021/acs.energyfuels.6b01151.

Hawthorne, S.B., Jin, L., Kurz, B.A., Miller, D.J., Grabanski, C.B., Sorensen, J.A., Pekot, L.J., Bosshart, N.W., Smith, S.A., Burton-Kelly, M.E., Heebink, L.V., 2017. Integrating petrographic and petrophysical analyses with CO_2 permeation and oil extraction and recovery in the Bakken tight oil formation. In: SPE Unconventional Resources Conference. https://doi.org/10.2118/185081-MS.

Hawthorne, S.B., Miller, D.J., Jin, L., Azzolina, N.A., Hamling, J.A., Gorecki, C.D., 2018. Lab and reservoir study of produced hydrocarbon molecular weight selectivity during CO_2-enhanced oil recovery. Energy Fuel. 32 (9), 9070–9080. https://doi.org/10.1021/acs.energyfuels.8b01645.

Hawthorne, S.B., Miller, D.J., Grabanski, C.B., Jin, L., 2020. Experimental determinations of minimum miscibility pressures using hydrocarbon gases and CO_2 for crude oils from the Bakken and cut bank oil reservoirs. Energy Fuel. 34 (5), 6148–6157. https://doi.org/10.1021/acs.energyfuels.0c00570.

Hawthorne, S.B., Grabanski, C.B., Jin, L., Bosshart, N.W., Miller, D.J., 2021. Comparison of CO_2 and produced gas hydrocarbons to recover crude oil from Williston Basin shale and Mudrock cores at 10.3, 17.2, and 34.5 MPa and 110 °C. Energy Fuel. 35 (8), 6658–6672. https://doi.org/10.1021/acs.energyfuels.1c00412.

He, Y., Qiao, Y., Qin, J., Tang, Y., Wang, Y., Chai, Z., 2022. A novel method to enhance oil recovery by inter-fracture injection and production through the same multi-fractured horizontal well. J. Energy Resour. Technol. 144 (4), 043005. https://doi.org/10.1115/1.4051623.

Hoffman, B.T., 2012. Comparison of various gases for enhanced recovery from shale oil reservoirs. In: SPE Improved Oil Recovery Symposium. https://doi.org/10.2118/154329-MS.

Hoffman, B.T., 2018. Huff-n-puff gas injection pilot projects in the Eagle Ford. In: SPE Canada Unconventional Resources Conference. https://doi.org/10.2118/189816-MS.

Hoffman, B.T., Evans, J.G., 2016. Improved oil recovery IOR pilot projects in the Bakken Formation. In: SPE Low Perm Symposium. https://doi.org/10.2118/180270-MS.

Jia, B., Jin, L., Mibeck, B.A., Smith, S.A., Sorensen, J.A., 2020. An integrated approach of measuring permeability of naturally fractured shale. J. Petrol. Sci. Eng. 186, 106716. https://doi.org/10.1016/j.petrol.2019.106716.

Jia, B., Jin, L., Smith, S.A., Bosshart, N.W., 2021. Extension of the gas research institute (GRI) method to measure the permeability of tight rocks. J. Nat. Gas Sci. Eng. 91, 103756. https://doi.org/10.1016/j.jngse.2020.103756.

Jin, L., Hawthorne, S., Sorensen, J., Kurz, B., Pekot, L., Smith, S., Bosshart, N., Azenkeng, A., Gorecki, C., Harju, J., 2016. A systematic investigation of gas-based improved oil recovery technologies for the Bakken tight oil formation. In: SPE/AAPG/SEG Unconventional Resources Technology Conference. https://doi.org/10.15530/URTEC-2016-2433692.

Jin, L., Sorensen, J.A., Hawthorne, S.B., Smith, S.A., Pekot, L.J., Bosshart, N.W., Burton-Kelly, M.E., Miller, D.J., Grabanski, C.B., Gorecki, C.D., Steadman, E.N., 2017a. Improving oil recovery by use of carbon dioxide in the Bakken unconventional system—a laboratory investigation. SPE Reservoir Eval. Eng. 20 (3), 602–612. https://doi.org/10.2118/178948-PA.

Jin, L., Hawthorne, S., Sorensen, J., Pekot, L., Kurz, B., Smith, S., Heebink, L., Herdegen, V., Bosshart, N., Torres, J., Dalkhaa, C., Peterson, K., Gorecki, C., Steadman, E., Harju, J., 2017b. Advancing CO_2 enhanced oil recovery and storage in unconventional oil play—experimental studies on Bakken shales. Appl. Energy 208, 171–183. https://doi.org/10.1016/j.apenergy.2017.10.054.

Jin, L., Pekot, L.J., Hawthorne, S.B., Salako, O., Peterson, K.J., Bosshart, N.W., Jiang, T., Hamling, J.A., Gorecki, C.D., 2018a. Evaluation of recycle gas injection on CO_2 enhanced oil recovery and associated storage performance. Int. J. Greenh. Gas Control 75, 151–161. https://doi.org/10.1016/j.ijggc.2018.06.001.

Jin, L., Pekot, L.J., Smith, S.A., Salako, O., Peterson, K.J., Bosshart, N.W., Hamling, J.A., Mibeck, B.A., Hurley, J.P., Beddoe, C.J., Gorecki, C.D., 2018b. Effects of gas relative permeability hysteresis and solubility on associated CO_2 storage performance. Int. J. Greenh. Gas Control 75, 140–150. https://doi.org/10.1016/j.ijggc.2018.06.002.

Jin, L., Wan, X., Azzolina, N.A., Bosshart, N.W., Zhao, J., Yu, Y., Yu, X., Smith, S.A., Sorensen, J.A., Gorecki, C.D., 2022a. Optimizing conformance control for gas injection EOR in unconventional reservoirs. Fuel 324 (2022), 124523. https://doi.org/10.1016/j.fuel.2022.124523.

Jin, L., Kurz, B.A., Ardali, M., Wan, X., Zhao, J., He, J., Hawthorne, S.B., Djezzar, A.B., Yu, Y., Morris, D., 2022b. Investigation of produced gas injection in the Bakken for enhanced oil recovery considering well interference. In: Unconventional Resources Technology Conference (URTeC). https://doi.org/10.15530/urtec-2022-3723697. URTeC-3723697.

Kias, E., Maharidge, R., Hurt, R., 2015. Mechanical versus mineralogical brittleness indicesacross various shale plays. In: SPE Annual Technical Conference and Exhibition. https://doi.org/10.2118/174781-MS.

Kumar, S., Mandal, A., 2017. A comprehensive review on chemically enhanced water alternating gas/CO_2 (CEWAG) injection for enhanced oil recovery. J. Petrol. Sci. Eng. 157, 696–715. https://doi.org/10.1016/j.petrol.2017.07.066.

Lee, S.H., Lough, M.F., Jensen, C.L., 2001. Hierarchical modeling of flow in naturally fractured formations with multiple length scales. Water Resour. Res. 37 (3), 443–455. https://doi.org/10.1016/j.petrol.2017.07.066.

Li, C., Pu, H., Zhao, J.X., 2019. Molecular simulation study on the volume swelling and the viscosity reduction of *n*-alkane/CO_2 systems. Ind. Eng. Chem. Res. 58 (20), 8871–8877. https://doi.org/10.1021/acs.iecr.9b01268.

Li, L., Lee, S.H., 2008. Efficient field-scale simulation of black oil in a naturally fractured reservoir through discrete fracture networks and homogenized media. SPE Reservoir Eval. Eng. 11 (4), 750–758. https://doi.org/10.2118/103901-PA.

Litvak, M.L., Nagarajan, N.R., Prasad, R.S., Shaarawi, K., 2020. Successful field test of enhancing Bakken oil recovery with propane injection Part II. development and application of innovative simulation technology. In: SPE/AAPG/SEG Unconventional Resources Technology Conference. https://doi.org/10.15530/urtec-2020-2775.

Liu, C., 2021. Automatic History Matching with Data Integration for Unconventional Reservoirs. The University of Texas at Austin, Austin, Texas. URL. https://hdl.handle.net/2152/89262.

Liu, C., Wu, K., Wu, J., Chang, C., Yang, X., Gong, Y., Zhao, E., Yu, W., Sepehrnoori, K., 2022. An accurate and efficient fracture propagation model auto-calibration workflow for unconventional reservoirs. In: SPE/AAPG/SEG Unconventional Resources Technology Conference. https://doi.org/10.15530/urtec-2022-3720957.

Malo, S., McNamara, J., Volkmer, N., Amirian, E., 2019. Eagle Ford—introducing the big bad wolf. In: Unconventional Resources Technology Conference. https://doi.org/10.15530/urtec-2019-624.

Mba, K., Prasad, M., 2010. Mineralogy and its contribution to anisotropy and kerogen stiffness variations with maturity in the Bakken Shales. In: SEG Annual Meeting. https://doi.org/10.1190/1.3513383, 2010.

Mirzaei, M., Cipolla, C.L., 2012. A workflow for modeling and simulation of hydraulic fractures in unconventional gas reservoirs. In: SPE Middle East Unconventional

Gas Conference and Exhibition. https://doi.org/10.2118/153022-MS.
Moinfar, A., Varavei, A., Sepehrnoori, K., Johns, R.T., 2013. Development of a coupled dual continuum and discrete fracture model for the simulation of unconventional reservoirs. In: SPE Reservoir Simulation Symposium. https://doi.org/10.2118/163647-MS.
Nagarajan, N.R., Stoll, D., Litvak, M.L., Prasad, R.S., Shaarawi, K., 2020. Successful field test of enhancing Bakken oil recovery by propane injection—Part I. field test planning, operations, surveillance, and results. In: SPE/AAPG/SEG Unconventional Resources Technology Conference. https://doi.org/10.15530/urtec-2020-2768.
Ozowe, W., Zheng, S., Sharma, M., 2020. Selection of hydrocarbon gas for huff-n-puff IOR in shale oil reservoirs. J. Petrol. Sci. Eng. 195, 107683. https://doi.org/10.1016/j.petrol.2020.107683.
Pankaj, P., Mukisa, H., Solovyeva, I., Xue, H., 2018. Enhanced oil recovery in Eagle Ford: Opportunities using huff-N-puff Technique in unconventional reservoirs.. In: SPE Liquids-Rich Basins Conference-North America https://doi.org/10.2118/191780-MS.
Pearson, C.M., Griffin, L.G., Strickland, S.L., Weddle, P.M., 2018. Twelve years and twelve thousand multi-stage horizontal wells in the Bakken—how is industry continuing to increase the cumulative production per well?. In: SPE International Hydraulic Fracturing Technology Conference and Exhibition https://doi.org/10.2118/191455-18IHFT-MS.
Pitman, J.K., Price, L.C., LeFever, J.A., 2001. In: Diagenesis and Fracture Development in the Bakken Formation, Williston Basin. Implications for Reservoir Quality in the Middle Member (No. 1653). US Department of the Interior. US Geological Survey. https://doi.org/10.3133/pp1653.
Pospisil, G., Weddle, P., Strickland, S., McChesney, J., Tompkins, K., Neuroth, T., Pearson, M., Griffin, L., Kaier, T., Sorensen, J., Jin, L., Jiang, T., Pekot, L., Bosshart, N., Hawthorne, S., 2020. Report on the first rich gas EOR cyclic multiwell huff 'n' puff pilot in the Bakken tight oil play. In: SPE Annual Technical Conference and Exhibition. https://doi.org/10.2118/201471-MS.
Rivero, J.T., Jin, L., Bosshart, N., Pekot, L.J., Sorensen, J.A., Peterson, K., Anderson, P., Hawthorne, S.B., 2018. Multiscale modeling to evaluate the mechanisms controlling CO_2-based enhanced oil recovery and CO_2 storage in the Bakken Formation. In: SPE/AAPG/SEG Unconventional Resources Technology Conference. https://doi.org/10.15530/URTEC-2018-2902837.
Salako, O., Jin, L., Barajas-Olalde, C., Hamling, J.A., Gorecki, C.D., 2018. Implementing adaptive scaling and dynamic well-tie for quantitative 4-D seismic evaluation of a reservoir subjected to CO_2 enhanced oil recovery and associated storage. Int. J. Greenh. Gas Control 78, 306–326. https://doi.org/10.1016/j.ijggc.2018.08.015.
Shoaib, S., Hoffman, B.T., 2009. CO_2 flooding the elm coulee field. In: SPE Rocky Mountain Petroleum Technology Conference. https://doi.org/10.2118/123176-MS.
Smith, M.G., Bustin, R.M., 1995. Sedimentology of the Late Devonian and Early Mississippian Bakken Formation, Williston Basin. Seventh International Williston Basin Symposium, pp. 103–114.
Smith, S.A., Mibeck, B.A., Hurley, J.P., Beddoe, C.J., Jin, L., Hamling, J.A., Gorecki, C.D., 2018. Laboratory determination of oil draining CO_2 hysteresis effects during multiple floods of a conventional clastic oil reservoir. Int. J. Greenh. Gas Control 78, 1–6. https://doi.org/10.1016/j.ijggc.2018.06.019.
Sorensen, J., Hamling, J., 2015. Enhanced Oil Recovery (EOR) in Tight Oil—Lessons Learned from Pilot Tests in the Bakken. Tight Oil Optimization Workshop (Calgary, Alberta, Canada).
Sorensen, J.A., Kurz, B.A., Hawthorne, S.B., Jin, L., Smith, S.A., Azenkeng, A., 2017. Laboratory characterization and modeling to examine CO_2 storage and enhanced oil recovery in an unconventional tight oil formation. Energy Proc. 114, 5460–5478. https://doi.org/10.1016/j.egypro.2017.03.1690.
Sorensen, J.A., Pekot, L.J., Torres, J.A., Jin, L., Hawthorne, S.B., Smith, S.A., Jacobson, L.L., Doll, T.E., 2018. Field test of CO_2 injection in a vertical Middle Bakken well to evaluate the potential for enhanced oil recovery and CO_2 storage. In: SPE/AAPG/SEG Unconventional Resources Technology Conference. https://doi.org/10.15530/URTEC-2018-2902813.
Torres, M.X.F., Yu, W., Ganjdanesh, R., Kerr, E., Sepehrnoori, K., Miao, J., Ambrose, R., 2019. Modeling interwell fracture interference and huff-n-puff pressure containment in Eagle Ford using EDFM. In: SPE Oklahoma City Oil and Gas Symposium. https://doi.org/10.2118/195240-MS.
Wan, X., 2020. Coupled Simulation of Hydraulic Fracturing, Production, and Refracturing for Unconventional Reservoirs. Doctoral Dissertation. The University of North Dakota.
Wan, X., Rasouli, V., Damjanac, B., Yu, W., Xie, H., Li, N., Rabiei, M., Miao, J., Liu, M., 2020. Coupling of fracture model with reservoir simulation to simulate shale gas production with complex fractures and nanopores. J. Petrol. Sci. Eng. 193, 107422. https://doi.org/10.1016/j.petrol.2020.107422.
Wan, X., Jin, L., Azzolina, N.A., Butler, S.K., Yu, X., Zhao, J., 2022. Applying reservoir simulation and artificial intelligence algorithms to optimize fracture characterization and CO_2 enhanced oil recovery in unconventional reservoirs: a case study in the Wolfcamp Formation. Energies 15, 8266. https://doi.org/10.3390/en15218266, 2022.
Wang, X., Luo, P., Er, V., Huang, S., 2010. Assessment of CO_2 flooding potential for Bakken Formation, saskatchewan. In: Canadian Unconventional Resources and International Petroleum Conference. https://doi.org/10.2118/137728-MS.
Warren, J.E., Root, P.J., 1963. The behavior of naturally fractured reservoirs. SPE J. 3 (3), 245–255. https://doi.org/10.2118/426-PA.
Xu, Y., 2015. Implementation and Application of the Embedded Discrete Fracture Model (EDFM) for Reservoir Simulation in Fractured Reservoirs. Master Thesis. The University of Texas at Austin, Austin, Texas. URL. http://hdl.handle.net/2152/34216.
Xu, Y., Cavalcante Filho, J.S.A., Yu, W., Sepehrnoori, K., 2017. Discrete-fracture modeling of complex hydraulic-fracture geometries in reservoir simulators. SPE Reservoir Eval. Eng. 20 (2), 403–422. https://doi.org/10.2118/183647-PA.
Yu, W., Sepehrnoori, K., 2014. Optimization of well spacing for Bakken tight oil reservoirs. In: SPE/AAPG/SEG Unconventional Resources Technology Conference. https://doi.org/10.15530/URTEC-2014-1922108.
Yu, W., Fiallos Torres, M.X., Liu, C., Miao, J., Sepehrnoori, K., 2020. Complex fracture hits modeling and analysis for parent-child wells in Eagle Ford. In: SPE Annual Technical Conference and Exhibition. https://doi.org/10.2118/201455-MS.
Yu, W., Javadpour, F., Varavei, A., Sepehrnoori, K., 2014. Sensitivity analysis of hydraulic fracture geometry in shale gas reservoirs. J. Petrol. Sci. Eng. 113, 1–7. https://doi.org/10.1016/j.petrol.2013.12.005.
Zhang, S., Jia, B., Zhao, J., Pu, H., 2021. A diffuse layer model for hydrocarbon mass transfer between pores and organic matter for supercritical CO_2 injection and sequestration in shale. Chem. Eng. J. 406, 126746. https://doi.org/10.1016/j.cej.2020.126746.
Zhao, J., Jin, L., Azzolina, N.A., Wan, X., Yu, X., Sorensen, J.A., Kurz, B.A., Bosshart, N.W., Smith, S.A., Wu, C., Vrtis, J.L., Gorecki, C.D., Ling, K., 2022. Investigating enhanced oil recovery in unconventional reservoirs based on field cases review, laboratory and simulation studies. Energy Fuels 36 (24), 14771–14788. https://doi.org/10.1021/acs.energyfuels.2c03056, 2022.